

# Cellulose

## Comparison of cellulose nanocrystals obtained by sulfuric acid hydrolysis and ammonium persulfate treatment, intended as coating onto flexible food packaging materials

--Manuscript Draft--

<b>Manuscript Number:</b>	CELS-D-15-00434R1
<b>Full Title:</b>	Comparison of cellulose nanocrystals obtained by sulfuric acid hydrolysis and ammonium persulfate treatment, intended as coating onto flexible food packaging materials
<b>Article Type:</b>	Original Research
<b>Keywords:</b>	Cellulose Nanocrystals, Ammonium Persulfate, Oxygen permeability, Film Coating
<b>Corresponding Author:</b>	Luciano Piergiovanni Universita degli Studi di Milano Milan, Mi ITALY
<b>Corresponding Author Secondary Information:</b>	
<b>Corresponding Author's Institution:</b>	Universita degli Studi di Milano
<b>Corresponding Author's Secondary Institution:</b>	
<b>First Author:</b>	Erika Mascheroni, PhD
<b>First Author Secondary Information:</b>	
<b>Order of Authors:</b>	Erika Mascheroni, PhD Riccardo Rampazzo, MS Marco Aldo Orteni, PhD Giulio Piva, MS Simone Bonetti, MS Luciano Piergiovanni
<b>Order of Authors Secondary Information:</b>	
<b>Funding Information:</b>	
<b>Abstract:</b>	<p>Cellulose nanocrystals (CNCs), extracted from trees, plants, or other cellulose-containing species, can be used in combination with other materials to improve their performance or introduce new potentialities; their preparation usually involves a chemical acid hydrolysis process intended to dissolve amorphous chains from the cellulose fibers to release crystal domains. In this work the morphological and chemical characterization of CNCs produced from cotton linters through two different processes, the common acidic hydrolysis (H<sub>2</sub>SO<sub>4</sub>) and a less investigated ammonium persulfate treatment (APS), was carried out; the main purpose was to compare and understand the potentialities of using these two types of CNCs as coatings for Poly(ethylene terephthalate) (PET) film. CNCs produced by APS treatment showed higher charge density due to the carboxylic groups formed during the process, more clarity of the solution and, as a consequence, higher transparency of the coating, but similar crystallinity pattern; these peculiarities confer higher oxygen barrier respect to the CNCs produced by H<sub>2</sub>SO<sub>4</sub> treatment, and the availability of active sites for potential surface modification or chemical grafting. Anyway, both CNCs coatings showed oxygen permeability coefficient lower than synthetic resins commonly used in flexible packaging, they did not affect significantly the optical properties of the substrate and revealed good coefficients of friction. The use of such nanocellulose as water based coating can be considered a possible alternative to conventional food packaging materials: due to the moisture sensitivity of the coating and due to the no sealable property, as happens for EVOH or PVOH oxygen barrier synthetic resins, this type of</p>

	<p>material need to be laminated with another plastic layer such as a polyolefin. In this case it might enhance the final properties of packaging solutions for perishable food products, while reducing their environmental impact with a thin layer of a bio-based polymer.</p>
<p><b>Response to Reviewers:</b></p>	<p>Responses to Reviewers</p> <p>Ms. Ref. No.: CELS-D-15-00434</p> <p>Title: Comparison of cellulose nanocrystals obtained by sulfuric acid hydrolysis and ammonium persulfate treatment, intended as coating onto flexible food packaging materials</p> <p>Thank you for the editor-in-chief and reviewer's constructive comments that contribute to improve the overall quality of our manuscript. We have taken into consideration all the remarks assigned and we tried to incorporate major revisions as suggested. We hope that the revised manuscript will be favourably reconsidered for publication. The answers to the comments are reported in italic in the following paragraph.</p> <p>COMMENTS FOR THE AUTHOR:</p> <p>Editor-in-Chief: We are asking all authors to use the conventions for the Miller indices described in French, Cellulose 21:885-896 (2014). It would be interesting to test your peak deconvolution method on a calculated diffraction pattern, as described in that paper.</p> <p>The authors wish to thank the Editor for the important remark that, together with the specific comment of the reviewer 2 (Line 85) concerning the classical model of crystallinity of the CNCs, led us to study into deep the question concerning the evaluation of the crystallinity of the CNCs.</p> <p>As suggested by the Editor, we decided to use the conventions for the Miller indices. We reported in Figure 3 the powder diffraction patterns calculated with Mercury software in comparison with the experimental data for CNCs from APS and CNCs from H2SO4. The powder diffraction patterns were calculated on the basis of the published atomic coordinates and unit cell dimensions contained in the modified "Crystal information files" (.cif).</p> <p>It is possible to observe in Figure 3 that CNCs have a diffraction pattern more similar to the cellulose I<math>\beta</math> crystal structure with the three main peaks for the I<math>\beta</math> one-chain triclinic unit cell with the Miller Index of (1-10) (110) and (200). The differences in the peak widths correspond to different crystallite sizes. The size can be assessed with the Scherrer equation. We decided to delete the data concerning the calculation of the degree of crystallinity obtained using the XRD analysis. As reported by French, Cellulose 21:885-896 (2014), on these simulated patterns, there is no modelling of amorphous scattering, so it is not appropriate to position a background intensity curve as high as minimum intensity at 18° 2<math>\theta</math>. For similar reason the calculation of the degree of crystallinity with the deconvolution method of the same XRD spectra is not appropriate. CI in this case is indeed calculated from the ratio between the area of all crystalline peaks to the total area underneath the diffraction pattern. By this approach, several assumptions about correlation between peak broadening and amorphous contribution are necessary and still under vivid debate. The authors prefer to use the XRD results to stress the self-evident quality of the CNCs obtained. A more common notion of "Degree of crystallinity" is given by NMR analysis (with the Lorentzian functions used to perform the deconvolution of the C4 peaks), providing the relative masses of crystalline and amorphous material in a given sample. Such a method was used in the paper to fulfill the requests of the reviewers.</p> <p>Reviewer #1: This manuscript reported cellulose nanocrystals prepared by H2SO4 hydrolysis and by APS treatment. The morphology, crystallinity, chemical and thermal</p>

properties, charge density as well as surface energy of the two types of CNCs were studied and compared. The application of CNCs as barrier films for food packaging were also investigated. Overall, the manuscript is well conceived and written. The authors have done thorough characterizations to compare CNCs produced by two processes. The science is sound and the topic is interesting to the field of nanocellulose. Several minor revisions are suggested that the authors may consider addressing.

Page 19. Line 441-442. FTIR of CNCs by APS treatment has two peaks around 1700 cm<sup>-1</sup>. It will be helpful to assign both peaks.

The two peak around 1700 cm<sup>-1</sup> were identified. FTIR spectra of the different CNCs show distinct  $\nu(\text{C}=\text{O})$  stretching peaks from 1735 cm<sup>-1</sup> assigned to the COOH, 1613 cm<sup>-1</sup> assigned to the COO<sup>-</sup> Na<sup>+</sup> and around 1630 cm<sup>-1</sup> assigned to the COO-NH<sub>4</sub><sup>+</sup> respectively as reported in literature in Lam et al., 2013. In this specific case we tested, with the FTIR technique, the CNCs in acidic form (pH=2), so we are able to identify the COOH peak (1735 cm<sup>-1</sup>) and the peak of COO-NH<sub>4</sub><sup>+</sup> (1630 cm<sup>-1</sup>).

Page 19. Table 4. It is suggested to include the clarity of CNCs in water dispersion produced by two processes and correlate with charge density and transparency of the films (table 6).

In agreement with the reviewer's remark, we added the clarity of the CNCs water solution at 7% w/w after ultrasound treatment for 15 minutes (0.7 cycles, 70% output). The clarity was measured as turbidity of the solution using a spectrophotometer at  $\lambda=600\text{nm}$ . The results show that turbidity of the APS solution is lower than the H<sub>2</sub>SO<sub>4</sub> one and this could be related with surface charge density. Indeed, in the case of APS solution, the higher surface charge density induces a more efficient electrostatic interactions with water (i.e. a tighter hydrogen bonds network), leading to more stable CNCs dispersion. After solution deposition on the substrate, the strong capillary and surface forces due to drying and adsorption trigger a rearrangement of the crystal structure. As indicated also by the second reviewer, cellulose is known to have a very high transparency in solid non-porous form. In this case, we are in presence of a decrease of transparency of the PET film (the support) and this decrease is lower in the case of CNCs from APS treatment. Moreover, SEM micrographs recorded with 180KX Magnification showed homogenous surface of the coating with the presence of some holes, causing a more pronounced roughness in CNCs H<sub>2</sub>SO<sub>4</sub> coating than in APS.

In our opinion this set of data fulfills the reviewer's requests shedding a deeper light with respect to the pristine manuscript, strongly supporting our hypothesis as well.

Figure 2. TEM images with same magnification are suggested for better comparison of dimensions of CNCs produced by two treatments.

In agreement with the reviewer remark, the figures were selected with the same magnification for a better comparison of the CNCs

Reviewer #2: Referee comments on Mascheroni et al.'s "Comparison of cellulose nanocrystals obtained by sulfuric acid hydrolysis and ammonium persulfate treatment, intended as coating onto flexible food packaging materials"

The authors have produced cellulose nanocrystals (CNCs) by two different protocols; the "traditional" sulphuric acid approach and a newer approach based on oxidation with ammonium persulfate (APS). The two CNCs were then characterised and used as coatings on PET. Studies on newly developed chemical protocols are always needed and are of interest. However, I think the authors need to better emphasise what missing piece of information they want to add with this manuscript. If this had been the first time APS had been used for making CNCs, I would have voted for major revision. However, since there already are publications on this protocol, as the authors also mention, I judge this manuscript as borderline between major revision and reject (and resubmit). Since I am absolutely positive that the authors will try to have the manuscript published, in Cellulose or elsewhere, I have listed a few things to that I believe need to be addressed to have this manuscript published.

General 1. Improve the "packaging". In the introduction the authors need to better emphasise on what knowledge gap this manuscript is intended to fill, i.e. why this is interesting for our society and not just a report of experimental results. Both style and language should also be improved. If a thorough proof reading is not enough, the authors are encouraged to subject the manuscript to professional linguistic review.

We added two sentences at the end of Introduction to better emphasize the most important goal of this work, in relation to the packaging sector needs. The chance of producing CNCs from largely available biomass, as well as from industrial byproducts, by a procedure able to remove lignin and that does not need special pre-treatments, can open new frontiers in coating technology of flexible packaging materials. Preliminarily, however, we wanted to check possible differences between CNCs produced by conventional acidic hydrolysis and the APS process, and this comparison is the main target of this paper.

General 2. Numbers are in general given with several decimals. I doubt that they always are significant? When values are given with errors, it is also preferable to inform the reader if they are standard deviations or confidence limits, and on what data they are based. I cannot always find how many measurements that were performed. Write this in the caption of the figure or table, or in Methods.

According to the reviewer remark, we reconsidered the data and we let only the number of decimal essential to compare the different CNCs. All values are reported with standard deviation indicated in the text ad SD

Line 23: (CNC) should read (CNCs).  
The word CNC has been changed in CNCs

Line 34: avoid formulations as "a little higher".  
The term has been delated

Line 52: "cellulose nanofibrils (NFCs)" should read "cellulose nanofibrils (CNFs)".  
The word NFCs has been changed with CNFs

Lines 53-57: There are studies on CNFs that show that it is advantageous to keep the hemicelluloses (e.g. Galland et al. Biomacromolecules 2015, DOI: 10.1021/acs.biomac.5b00678).

Unfortunately, when we wrote the paper, we were not aware of the article of Galland et al. It is definitely pertinent to the subject and, therefore, we added the new citation and a comment

Line 67: There are others that have used periodate, for example Yang et al. Langmuir 2012, who I believe also filed a patent on this. There are also other chemistries that can follow the periodate oxidation.

According to the reviewer's suggestions about lines 67 and 69, we have restructured the initial part of Introduction and inserted two pertinent citations (Yang et al. 2013 - Chinga-Carrasco and Syverud 2014)

Line 69: Carboxymethylation might also deserve being mentioned.  
See above

Line 77: The abbreviation NFCs (which should be CNFs) has already been defined on line 52.

Ok correct

Line 85: The classical model is that cellulose is arranged in crystalline and amorphous regions. However, this model is highly debated! As far as I know there is no experimental evidence that support this model and I suggest that you do not use it. In agreement with this remark, the authors analyzed in a better way the literature, in particular the articles published on "Cellulose". The authors referred to the model presented in literature, for example in the article on Carbohydrate Polymers 83 (2011) 1740–1748 Water sorption behavior and gas barrier properties of cellulose whiskers and microfibrils films by the authors Belbekhouche, S. Bras J, Siqueira G, Chappey C Lebrun L, Khelifi B, Marais S and , Dufresne A.

Other articles published on Cellulose and more focused on the crystallinity structure of cellulose investigated the issue more deeply and surely it is possible to assess that the question of cellulose structure is highly debated. In particular in Nishiyama Y, Structure and properties of the cellulose microfibril Journal of Wood Science (2009), 55: 241-249 the structure of microfibril is presented and discussed. The article reports that cellulose microfibril can be considered as a single thin and long crystalline entity with highly anisotropic physical properties and the two models (series model and microfibril model) are compared and discussed. Also in two other articles (Nishiyama Y, Johnson GP and French AD Diffraction from nonperiodic models of cellulose crystals, Cellulose 2012 19:319-336 and Nishiyama Y, Kim UJ, Kim DY, Katsumata KS, May RP, Lagan P. Periodic disorder along ramie cellulose microfibrils. Biomacromolecules, 2003: 4, 1013-1017) it is reported that observation by microscopy hypothesis on the morphogenesis, and molecular modeling often lead to structural models that do not necessarily fit the simplistic two-phase model. Cellulose is thought to crystallize in proximity to the polymerization site where many chains are simultaneously produced and deposited, leading to a continuous, fine but crystalline filament. In this filaments, no amorphous regions have been observed, and disordered, or strained regions seems to be very small with the presence of periodic defects. The measurement of chemical reactivity shows the rupture of hydrogen bonding O3H-O5(of the ring) only in this region of defect.  
The text was so modified according to these knowledges.

Line 131: I assume that the expression "elongated voids" refers to the lumen of the fibre.

Yes, the technical word for cellulose matrix is "Lumen of the fiber". So the text was corrected

Line 161: CNC should read CNCs.

Ok it has been corrected.

Line 188: What do the authors mean with "to avoid decomposition or burning"?

Cellulose will not burn at this temperature. The standard way to determine dry content of cellulosic fibres is to dry them overnight at 105 °C.

The observation of the reviewer is right, the official method to determine the dry content is to put the sample at 105°C overnight. The text was corrected

Line 192: Why was the dispersion freeze dried? Would this not only generate a problem to re-disperse the CNCs?

The authors would like to explain the reason of the freeze drying treatment. The production was done on laboratory scale and the variables that are inserted time by time, for a research approach, are not able to guarantee always the same dry content for each production. For the coating application, we needed solutions with the same concentration of CNCs so we prefer to dry the CNCs production. Even more, the authors have seen that the ultrasound treatment conditions of the CNCs solution are able to determine the final properties of the CNCs solution and, as a consequence, also of the coating. For these reasons, freeze dried product led us to modulate the final solution properties

Line 256: Why is 1.6 g/cm<sup>3</sup> used there and 1.58 g/cm<sup>3</sup> on line 319?

The text was corrected

Line 274: Hold the Alt key and type 0197 to produce an Å.

The text was corrected

Line 301: Here and on many other places in the text the authors cannot differentiate between the proper use of CNC and CNCs. Here it should be CNC. See my general comment about linguistic review.

The authors decided to use uniform style, so they will always use CNCs (plural form)

Line 307: Very short. How many samples and how many spots in each sample were evaluated?

The transmittance of the two different CNC coating was measured at 550 nm, according to the ASTM D 1746-70, by means of a Perkin-Elmer L650 UV-VIS spectro photometer. Each measure was replicated three times, by analyzing four spots, each

replica.

Line 312: Gravimetric determination is the best way to determine the thickness? This can only give an average and no indication on the structure and homogeneity of the coating. Cross-sections under SEM would presumably confirm the thickness and give additional information about the coating.

In agreement with the reviewer remark, cross section under SEM observation were done. The author agree with the comment of the reviewer that the method previously used by the author is not able to provide indication about the structure and the homogeneity of the coating. The authors decided to delete the data obtained with the weight method because this method require a precise estimation of CNCs density that we considered 1.6 g/cm<sup>3</sup>, a value currently found in literature attributed to the powder form of the CNC and probably it is not the density of the CNCs in form of coating. SEM observation permitted to verify, in fact, that the surface of the coating is homogeneous (the thickness was quite the same in different point of the surface) but the value was lower than the value obtained with the previous method, the reason could be an underestimation of the density. The values of the thickness for both the coating was around 450±50 nm. The text was corrected according to these results and a figure of SEM observation was inserted

Line 328: Odd choice of reference. A more obvious choice would be any edition of Crank's "Mathematics of diffusion". The authors should also be aware that this equation assumes two (or several) layers that in no way interact with each other, i.e. it neglects the interface between the PET and coating.

According to the reviewer's remark, the authors changed the citation and added a sentence to underline the assumption behind the equation

Line 330: "Strength of (wet) adhesion" is an odd title for this evaluation. Water resistance or something would be more suitable. Since the sample is wiped (wet) wear or abrasion resistance might be a fair description.

The authors agree completely with the reviewer remark, in this paper no measure of strength adhesion are presented but only a test of the water resistance of the CNCs. The aim was to test the reaction of the coating to the high humidity because it is well known the problem of cellulose water sensitivity

Line 377: "... to lead the quantitative obtainment of cellulose nanocrystals." Please rephrase.

The sentence was changed: "The two different processes used on the same batch of cotton linters were able to give cellulose nanocrystals that are characterized to see their peculiarities."

Line 399: avoid "perfectly matches".

The word perfectly was deleted

Table 2: With an error of 47 nm in length, there is no need what so ever to use two decimals on the average (110 nm)!! Furthermore, if simple error propagation is performed, the uncertainty of the L/d for APS is 8, i.e. from Table 2 it is impossible to with any certainty say that APS results in CNCs with higher aspect ratio!

The criticism is completely justified and the authors changed accordingly the table and the comments

Line 424: "little higher"... Neither evaluation technique shows any significant difference in crystallinity. Unless measurements were performed under inert gas, the indication of a difference could simply be due to different moisture content.

The author agree with the reviewer and also according to the Editor's suggestions, this part of the text was revised and the original Table 3 was deleted, leaving only the crystallinity value obtained by NMR analysis. The measurement were done under an inert gas, anyway the difference are not statistically significant as reported in the text..

Line 500: Omit + in CNC-COONa+, or write CNC-COO-Na+

Ok, it has been corrected with the second version

Line 518: Why is the coating reducing the transparency? Cellulose is known to have a



very high transparency in solid non-porous form. An increase in transparency or haze might come from particles that are large enough to scatter visible light, or from an increased surface roughness.

According to the reviewer's suggestion the authors explained the small increases of haze and the small reduction of transparency with a comment related to surface roughness (displayed by SEM observation) and the clarity of the CNCs solutions that was added in Table 5.

Line 524: avoid "huge".  
The word huge was deleted

Line 557: If this is a comparison between two types of CNCs, please describe why the APS process is better than sulphuric acid.

The authors have underlined many times in the text that CNCs obtained by the APS process seem different and better than CNCs produced by sulfuric acid hydrolysis, according to the final use to which they are intended. The nanocrystals from APS lead to a more transparent film, a lower COF, a more stable coating in a moist condition and, mostly, a higher barrier to oxygen permeation. Moreover, concerning the APS process, the authors underlined, with reference to the literature cited, the utility of a process that can be applied to lignin containing cellulose sources

Table 7: To really test the coatings from the two CNCs, I suggest that measurements are performed also at 80% RH, or even 90% RH. Table 7 shows that the permeability increases 6 times for sulphuric acid CNCs and 22 times for APS CNCs when the RH is increased from 0 to 50 %. This indicates that the sulphuric acid CNCs might be better than APS CNCs at higher (more relevant) humidities. Also, what is the reason behind the higher sensitivity? Is it only due to higher charge or is it something else?

These reviewer's comments are justified by the results presented. Therefore, the authors added the following sentence: The apparent higher moisture sensitivity of CNCs from the APS process, which shows a higher increase of permeability when measured at 50% RH in comparison with H<sub>2</sub>SO<sub>4</sub> CNCs coated film, is consistent with the higher wettability shown by optical contact angle evaluation (Table 5) and can be attributed to the higher charge density. In any case, the moisture sensitivity of the coating, as happens for the most common oxygen barrier synthetic resins (EVOH or PVOH), is overcome by the need of providing a sealable layer, thus polyolefinic and moisture barrier, to the possible final laminate in a real application.

Line 561: Shorten the discussion by moving some parts to Discussion.  
The authors removed about 80 words from the Conclusion

Line 581: Define in what way the APS coating is better, or at least under what conditions.

As the author stated in the conclusion: "...transparency, friction coefficient and wettability of the coating were always better for the CNCs coating obtained by the APS process, and especially the oxygen barrier property revealed as a very interesting and promising feature. Therefore, these advantages must be correlated to the efficacy of cellulose fragmentation and to the higher charge density due to the presence of carboxylic groups, which in turn gave rise to a more performing coating." Also, with reference to the APS process, the authors wrote in the conclusion that: "The use of ammonium persulfate to obtain cellulose nanocrystals has been initially proposed in order to perform in one single step a complete fragmentation of various cellulosic biomasses, in contrast to acid hydrolysis which requires pretreatment steps for cellulose isolation. This is a very important target that deserves to be fully explored to valorize largely available, renewable resources" The same arguments were reported along the discussion of results

Figure 1: No real need for this figure. If the authors want to show the structure, use this structure in a chemical reaction to simultaneously explain what happens when APS reacts with cellulose.

The figure was deleted

Figures 2 and 3: Use the images of same magnification.  
The figures were corrected and renamed Fig1a and Fig1b

Figure 4: What is meant by arbitrary units? Please read up on DLS. The y-axis should be intensity, number or volume, and all three mean different things. I suggest that signal intensity is used since it does not "filter away" the effect of larger particles. The figure was corrected using the signal intensity as suggested and renamed as Fig 3

Figure 5: Is this one single measurement or how many measurements were performed?

The authors performed three measurement and the curve can be stackable so just one curve was reported





## UNIVERSITÀ DEGLI STUDI DI MILANO

*Department of Food, Environmental and Nutritional Sciences*  
*Dipartimento di Scienze per gli Alimenti, la Nutrizione e l'Ambiente*



Dr. Alfred D. French, Editor-in-Chief, Cellulose,

Milan, 3<sup>rd</sup> November 2015

Dear Dr. French,

I am pleased to submit the revised copy of the original manuscript entitled “*Comparison of Cellulose nanocrystals obtained by Sulfuric acid hydrolysis and Ammonium persulfate treatment, intended as coating onto flexible food packaging materials*”, for possible publication as a research paper in *Cellulose*.

We very much appreciated the comments from the two referees that we found properly addressed. We tried to fulfil as much as possible their requests. According to the comments, we revised our manuscript writing in red all the changes operated in the manuscript. In the pages “Responses to Reviewers” we answered to all the questions raised by the referees and tried to explain our views. We confirm that this manuscript has not been published elsewhere in whole or in part and is not under consideration by another journal. Approvals of all of the Authors’ institutions have been granted to publish this work. All authors have approved the manuscript in this revised version and agree with submission to *Cellulose*.

The study was supported by our own funding. The authors have no conflicts of interest to. We have read and understood the "Ethical Responsibilities of Authors" in the journal’s “Instructions for Authors”, including the passage on screening for plagiarism with computer software.

Please address all correspondence to:

Luciano Piergiovanni  
DeFENS, Department of Food, Environmental and Nutritional Sciences – PackLAB  
Università degli Studi di Milano  
Via Celoria, 2 20133 MILAN, ITALY  
tel. + 39 02 50316638 fax + 39 02 50316672  
Luciano.Piergiovanni@unimi.it

We look forward to hearing from you at your earliest convenience.

Yours sincerely,



34 of the coating, but similar crystallinity pattern; these peculiarities confer higher  
35 oxygen barrier respect to the CNCs produced by H<sub>2</sub>SO<sub>4</sub> treatment, and the  
36 availability of active sites for potential surface modification or chemical grafting.  
37 Anyway, both CNCs coatings showed oxygen permeability coefficient lower than  
38 synthetic resins commonly used in flexible packaging, they did not affect  
39 significantly the optical properties of the substrate and revealed good coefficients  
40 of friction. The use of such nanocellulose as water based coating can be considered  
41 a possible alternative to conventional food packaging materials: due to the moisture  
42 sensitivity of the coating and due to the no sealable property, as happens for EVOH  
43 or PVOH oxygen barrier synthetic resins, this type of material need to be laminated  
44 with another plastic layer such as a polyolefin.  
45 In this case it might enhance the final properties of packaging solutions for  
46 perishable food products, while reducing their environmental impact with a thin  
47 layer of a bio-based polymer.

48 *Keywords: Cellulose Nanocrystals, Ammonium Persulfate, Oxygen permeability,*  
49 *Film coating*

50

51  
52  
53  
54  
55  
56  
57  
58  
59  
60  
61  
62  
63  
64  
65  
66  
67  
68  
69  
70  
71  
72  
73  
74  
75  
76  
77

## 1. INTRODUCTION

Cellulose, the most abundant natural polymer on the earth, can potentially become a widely used renewable nanomaterial for various applications in both its forms: cellulose nanocrystals (CNCs) and cellulose nanofibrils (CNFs) (Li et al. 2015; Dufresne 2012). Two main approaches are commonly used for obtaining cellulose nano-particles: mechanical treatments and acid hydrolysis, being the last the classical method for CNCs production.

For nanocellulose production by mechanical treatment, several variants and technological supports were proposed in the last 30 years (Moon et al. 2011; Rebouillat and Pla 2013; Nakagaito and Yano 2004; Berglund 2005). Besides the mechanical process of high-pressure homogenization, pre-treatments like further refining, oxidation by 2,2,6,6-tetramethylpiperidiny-1-oxyl, known as TEMPO, (Saito et al. 2007) or periodate-chlorite mixture (Liimatainen et al. 2012, Yang et al. 2013), enzymatic (Paakko et al. 2007), ultrasound treatment (Peng et al. 2010), combination of carboxymethylation and periodate oxidation (Chinga-Carrasco and Syverud 2014) have been used. The large number of hydrogen bonds among cellulose fibrils hinders the transverse cleavage required to obtain the nano-sized dimensions, rendering the processes to obtain nanocellulose difficult and variable according to the cellulose source used (Iwamoto et al. 2008). In addition, the plant-based raw materials (i.e. the most common cellulose sources) contain also hemicellulose, lignin, extractives and minerals, which have been considered hurdles to polymer fragmentation, to be thoroughly removed in order to obtain nanocellulose (Spence et al. 2011; Spence et al. 2010a; Spence et al. 2010b). More recently, however, Galland et al. (2015) demonstrated, in the preparation of CNFs by a mild peracetic acid delignification process, that highly preserved cellular molar

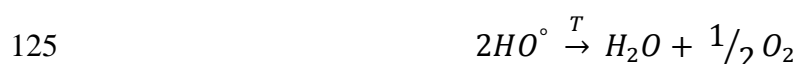
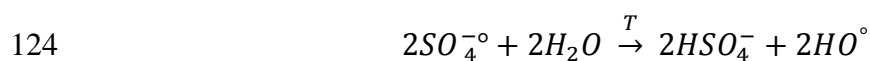
78 mass with up to 24% of hemicellulose content, contributes to CNF dispersion. This  
79 multistep process led to unique final properties and provided a possible physical  
80 model structure of the CNFs obtained. The cellulose oxidation, based on TEMPO,  
81 as well as on other chemicals, has been widely proposed in combination with acid  
82 hydrolysis or mechanical treatment, leading to effective transformation of cellulose  
83 hydroxyls groups into carboxyl. TEMPO oxidation, in particular, has been also  
84 proposed as an intermediate step in the grafting of various functional groups on  
85 cellulose chains (Araki et al. 2000), and in the enhancement of nanofibrils  
86 properties (Saito and Isogai 2007; Habibi et al. 2006). The different procedures in  
87 the mechanical treatment can produce cellulose nanofibrils with a broad range of  
88 morphologies and different performances. However, considering the different steps  
89 and the large number of variants, it is generally considered a high-energy  
90 demanding and time consuming process (Siro and Plackett 2010).

91 The production of nanocellulose by acid hydrolysis is the most classical procedure  
92 for cellulose fragmentation (Nickerson and Habrle 1947; Favier et al. 1995;  
93 Håkansson and Ahlgren 2005; Bondeson et al. 2006; Elazzouzi-Hafraoui et al.  
94 2008). The structure of cellulose is highly debated in the scientific field  
95 (Belbekhouche et al. 2011; Nishiyama et al. 2009), but the measure of chemical  
96 reactivity showed the rupture of hydrogen bonding between O3H and the ring  
97 oxygen O5 only in the region of defect that are periodically present along the  
98 microfibril and due to the biological synthesis of the cellulose (Nishiyama et al.  
99 2009). The dimensions and the morphologies of these particles mainly depend on  
100 the cellulose source and the process used. Different acids have been tested and used  
101 in nanocellulose production (sulfuric, hydrochloric, phosphoric, hydrobromic and  
102 maleic acid (Filpponen 2009; Filson and Dawson-Andoh 2009; Okano et al. 1999)  
103 leading to distinct properties and morphologies of CNCs. Concentrated sulfuric acid

104 is the most common medium for the hydrolysis process because it determines the  
105 formation of surface charged sulfate ester groups on the cellulose chains which  
106 promotes water dispersion of the nano-particles, avoiding the aggregation  
107 phenomena observed using hydrochloric acid (Araki et al. 2000). This process is  
108 easy to apply and low energy consuming but it can be time consuming, not  
109 ecofriendly and pretreatments are necessary starting from lignocellulosic matrices  
110 (Espino et al. 2014). This method indeed is not able to eliminate lignin,  
111 hemicelluloses and other impurities within plant raw materials.

112 An alternative to these processes is ammonium persulfate (APS) treatment (Leung  
113 et al. 2011). APS is a chemical widely used as strong oxidizer in polymer chemistry  
114 (Jayakrishnan and Shah 1984) as etchant, cleaning and bleaching agent in various  
115 industries (Turrentine 1906) and it has low long-term toxicity, high water solubility  
116 and low cost. Ammonium persulfate is generally preferred to potassium and sodium  
117 persulfates because of its higher solubility, lower pH, lower density and viscosity.  
118 Persulfates decompose thermally in aqueous solutions by two independent  
119 reactions, which occur simultaneously (Kolthoff and Miller 1951):

120 (A) an un-catalyzed reaction leading to the symmetrical rupture of the O-O bond  
121 and the formation of two sulfate free-radicals which disappear reacting with  
122 water and producing anion bisulfate and atomic oxygen;



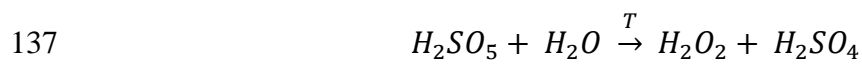
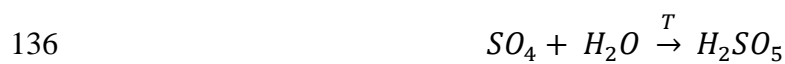
126 (B) an acid catalyzed reaction leading to the unsymmetrical rupture of the O-O  
127 bond to form sulfur tetroxide and bisulfate.







131 In diluted acidic solutions sulfur tetroxide decomposes to form atomic oxygen and  
132 sulfuric acid but if the acidic concentration increases (> 0.5M), the sulfur tetroxide  
133 reacts with water (Gall et al. 1943; Beer and Muller 1962) leading to mono  
134 peroxysulfuric acid (Caro's acid, H<sub>2</sub>SO<sub>5</sub>) which is patented as an effective  
135 delignification agent (Springer, Minor 1991).



138 Therefore, the uniqueness of this treatment is that a simultaneous hydrolysis and  
139 oxidation process of cellulose fibers occurs on the surface and within the inner  
140 amorphous regions due to the fast penetration of free radical ions (SO<sub>4</sub><sup>•-</sup>) and H<sub>2</sub>O<sub>2</sub>  
141 through the **lumen** of the fibers. In addition, the effectiveness of the phenomena is  
142 related to the progressive increase in acid concentration and peroxysulfuric acid  
143 generation.

144 Recent literature reports that APS is able to produce CNCs from different type of  
145 lignocellulosic materials containing up to 20% of lignin and the process has been  
146 patented as effective method to produce CNCs from renewable biomass (Leung et  
147 al. 2012; Leung et al. 2011). The reaction conditions (i.e. reaction time, temperature  
148 and APS concentration) can be tuned to have satisfactory yields and crystals with  
149 different aspect ratio. Moreover this treatment gives the opportunity to obtain  
150 carboxylated CNCs and to increase the crystallinity (Cheng et al. 2014). It is well  
151 known that carboxyl groups on the surface of the materials can provide active sites  
152 for template synthesis of nanoparticles, surface modification and chemical grafting  
153 (Ifuku et al. 2009; Qi et al. 2011; Arola et al. 2012). The oxidized cellulose obtained

154 by APS treatment shows a higher charge density that can improve interface  
155 interactions. Furthermore, the polymer crystallinity generally drives to better  
156 mechanical properties and higher gas barrier properties (Lasoski and Cobbs 1959;  
157 Salame 1989; Miller and Krochta 1997).

158 These peculiar characteristics of CNCs obtained by APS treatment and the huge  
159 availability of various **lignin containing** cellulose sources in agricultural biomasses  
160 **as well as in industrial byproducts**, addressed our research towards the potential  
161 uses of these carboxylated cellulose nanocrystals as coatings of novel, high  
162 performing and more sustainable flexible packaging materials (Li et al. 2013b; Li  
163 et al. 2013a). **A process able to make feasible the obtainment of large amount of**  
164 **CNCs from cheap and largely available sources, would be welcome by a sector,**  
165 **such as packaging materials production, requiring novel materials better performing**  
166 **and more sustainable, as coming from renewable sources. So far, however, to our**  
167 **best knowledge, does not exist an accurate comparison between CNCs obtained by**  
168 **the two processes and addressed to their potential use as coating for flexible**  
169 **packaging materials. Therefore**, in this paper we propose a comparison between the  
170 cellulose nanocrystals obtained by sulfuric acid hydrolysis and APS oxidation-  
171 hydrolysis starting from the same cotton linters, and a characterization of PET films  
172 coated with the two differently obtained CNCs, intended for food packaging  
173 applications.

174

175

## 176 2. MATERIALS AND METHODS

### 177 2.1 Materials

178 Cotton linters used as raw material to produce CNCs were kindly supplied by  
179 Innovhub (Milano, Italy). Sulfuric acid 96%, ammonium persulfate  $\geq 98\%$ ,

180 hydrochloric acid 37%, sodium hydroxide  $\geq 97\%$ , ion exchange resin Dowex  
181 Marathon MR-3 were purchased from Sigma-Aldrich (Milan, Italy).

182 Poly(ethylene terephthalate) (PET) film, having a thickness of  $12 \pm 0.5 \mu\text{m}$ , was  
183 provided by Sapici s.p.a (Cernusco sul Naviglio, Italy)

184

## 185 *2.2 CNC extraction by Sulfuric Acid hydrolysis*

186 Cellulose nanocrystals (CNCs) were obtained from cotton linters by a common  
187 procedure used by many Authors (Dong et al. 1996; Li et al. 2013b). Milled cotton  
188 linters were hydrolyzed by 64% w/w sulfuric acid under vigorous stirring at  $45^\circ\text{C}$   
189 for 45 minutes (fibers/acid ratio 1:17.5 g/mL). To quench the reaction, the mixture  
190 was diluted ten times with deionized water (18 M $\Omega$  cm, Millipore Milli-Q  
191 Purification System). The solution was centrifuged 5 times at 10000 rpm for 15  
192 minutes with addition of deionized water for each time in order to remove the excess  
193 of acid until the supernatant became turbid. For further purification, the centrifuged  
194 solution was posed inside dialysis tubes (Molecular Weight Cut off 12000 Da)  
195 immersed in deionized water for 72 hours to remove the acid still present and the  
196 low molecular weight contaminants. The suspension was then sonicated (UP 400S  
197 400 W, Hielscher ultrasonics GMBH, Teltow, Germany) repeatedly (cycles 0.7,  
198 time 5 minutes at 70% output) for bringing cellulose crystals to colloidal  
199 dimensions. During the ultrasonic treatment, the suspension was cooled with an ice  
200 water bath to avoid overheating. Ion exchange resin was added to the sonicated  
201 suspension (resin/solution ratio 10:1 g/L) to complex any residual ions. After that,  
202 the suspension was filtered under vacuum, using Munktell filter discs GF/C  $1.2 \mu\text{m}$   
203 in order to remove the largest fibers agglomerates and the microfibers possibly  
204 present. The cellulose content of the resulting aqueous suspension was determined  
205 by drying several samples (1 mL) at  $105^\circ\text{C}$  overnight. The pH of purified

206 suspensions was adjusted to 8 by 1M NaOH in order to gain fully charged CNCs.  
207 Secondly, the dispersion was frozen at -18 °C overnight and then moved to freeze  
208 dryer (LIO-10P, Cinquepascal, Trezzano s/N (MI), Italy). Finally, the freeze-dried  
209 powder obtained was stored in tightly close bottles under dry conditions.

210

### 211 *2.3 CNC extraction by Ammonium Persulfate treatment*

212 CNCs were produced from cotton linters by the hydrolyzing-oxidative method  
213 proposed by Leung and coworkers in 2011 (Leung et al. 2011). Milled cotton linters  
214 and 1M ammonium persulfate (APS) (ratio between fibers and APS 10:1 g/L) were  
215 introduced into a large beaker, onto a magnetic stirrer hotplate, equipped with a  
216 Vertex Digital thermoregulator (VELP Scientifica, Usmate (MB) Italy). The  
217 mixture was heated and continuously stirred at 75°C for 16 hour, limiting the  
218 evaporation by means of an aluminum foil cover. The suspension of CNCs obtained  
219 was centrifuged at 10000 rpm for 15 minutes with addition of deionized water in  
220 order to rinse the suspension. The centrifugation/washing procedure was repeated  
221 4 times until the suspension pH was around 4. In order to have the sodium form of  
222 CNCs, NaOH 1M was added until the suspension reached pH 8 and then it was  
223 sonicated for 15 minutes (0.7 cycles, 70% output). The purified suspension was  
224 frozen at -18 °C overnight and freeze-dried. Finally, the freeze-dried powder  
225 obtained was stored in tightly close bottles under dry conditions.

### 226 *2.4 Morphological characterization of CNCs*

227 Drops of aqueous dispersion of CNCs 0.5% w/w were deposited on carbon-coated  
228 electron microscope grids, negatively stained with uranyl acetate and allowed to  
229 dry. The samples were analyzed with a Hitachi Jeol-10084 transmission electron  
230 microscope (TEM) operated at an accelerating voltage of 80kV. Representative

231 micrographs have been selected for measuring the diameter and length of  
232 nanocrystals by digital image analysis (Image-Pro Plus software). The aspect ratio  
233 was also calculated. **Lengths average and diameters average of the crystals were**  
234 **determined by analyzing 70 crystals.**

235 In addition, the hydrodynamic size distributions of diluted aqueous dispersions of  
236 CNCs were determined by dynamic light scattering (DLS) (Malvern Instruments  
237 Nano Series Zetasizer optical units). Measurements were performed at  
238  $(23.0 \pm 0.1)^\circ\text{C}$  with a class 14 mW continuous wave He-Ne laser light ( $\lambda = 632.8$   
239 nm). The scatterers in solution are undergoing Brownian motions, constantly  
240 changing their instantaneous position and causing thus temporal fluctuations in the  
241 scattered light intensity. By applying correlation analysis and Stokes-Einstein  
242 relation, the hydrodynamic dimension and the size distribution of the scatterers can  
243 be calculated (Berne, Pecora 2000). Prior to DLS measurement the samples were  
244 diluted to 1:500 (w/w) with distilled water previously adjusted to pH 8 and  
245 maintained at  $25^\circ\text{C}$  under stirring until measurement. 1 ml of the diluted solution  
246 was injected in the measurement cell after 30 s homogenization with ultrasonic  
247 bath.

248 *2.5 Determination of the degree of oxidation (DO) of CNCs, charge density and*  
249 *clarity of the CNCs solutions.*

250 Conductometric titrations were performed to determine the carboxylic acid content  
251 of the CNCs. 50 mg of dry powders of CNCs were suspended into 15 mL 0.01M  
252 HCl for complete protonation of the COOH groups and sonicated for 10 min to  
253 disperse the nanocrystals. The CNCs suspensions were then titrated against 0.01M  
254 NaOH and the carboxylic acid contents were determined from the resulting

255 conductivity curves. The DO of the CNCs was calculated using the following  
256 equation:

$$257 \quad DO = \frac{162(V_2 - V_1)C}{w - 36(V_2 - V_1)C}$$

258 Where  $(V_2 - V_1)$  is the volume of NaOH (L) required to deprotonate the carboxylic  
259 acids groups, C is the concentration (M) of NaOH, w is the weight of the CNCs  
260 samples, the values 162 and 36 correspond to the molecular weight of an  
261 anhydroglucose unit (AGU) and the molecular weight difference between an AGU  
262 and sodium gluconate, respectively. The degree of oxidation (DO) was also  
263 quantified used FTIR spectra. FTIR spectroscopy was performed on Perkin Elmer  
264 instrument (Spectrum 100), equipped with ATR, at room temperature, **on CNCs in**  
265 **their acidic form (pH=2)**. The data were collected over 64 scans with a resolutions  
266 of  $4 \text{ cm}^{-1}$  and the DO was calculated by the ratio of the intensity of the carbonyl  
267 peak (absorbance bands at  $1735 \text{ cm}^{-1}$  ( $\nu(\text{C}=\text{O})$  in the acid form)) to that of the band  
268 near  $1060 \text{ cm}^{-1}$ , relating to the backbone structure of cellulose. The equation used  
269 in this case is the following:

$$270 \quad DO = 0.01 + 0.7(I_{1735} - I_{1060})$$

271 Surface charge density was estimated using the dimensions of CNC determined by  
272 TEM, assuming a cylindrical shape and a density of  $1.6 \text{ g/cm}^3$  for cellulose  
273 nanocrystals (Beck-Candanedo et al. 2005). **The clarity of the CNCs water solution**  
274 **at 7% w/w was also tested after ultrasound treatment for 15 minutes (0.7 cycles,**  
275 **70% output). It was measured as turbidity of the solution using a spectrophotometer**  
276 **at  $\lambda=600\text{nm}$ .**

277 *2.6 Crystallinity evaluation by Solid-state nuclear magnetic resonance (NMR)*  
278 *spectroscopy and by X-ray diffraction (XRD).*



279 All NMR spectra (three replication for each type of CNCs) were acquired at room  
280 temperature on a Bruker AVANCE-600 spectrometer (Bruker Spectrospin GmbH,  
281 Rheinstetten, Germany), equipped with a 4 mm broad-band CP-MAS probe for  
282 solid state measurements. About 100 mg of CNCs sample were directly pressed into  
283 a 4 mm ZrO<sub>2</sub> rotor without further treatment. <sup>13</sup>C spectra were acquired at 150.9  
284 MHz using Cross Polarization (CP) and Magic Angle Spinning (MAS) at 6-10 kHz  
285 (Pines et al. 1973). Proton decoupling was achieved with GARP-based composite  
286 pulse. Standard acquisition parameters were as follows: Spectral width: 75.7 kHz;  
287 acquisition time: 3.4 ms; relaxation delay: 2s (fast acquisition conditions); contact  
288 time for Cross Polarization: 1 ms; number of scans: 7000-24000. The contact time  
289 was optimized by systematic variation of the corresponding pulse within the 0.3-  
290 3.0 ms range. Adamantane was used as external chemical shift reference.

291 X-ray diffraction measures were conducted using an X-ray diffractometer (D8-  
292 Advance Bruker AXS GmbH) at room temperature with a monochromatic Cu-Kα  
293 radiation source (Wavelength 1.5418 Å ) in the step-scan mode with a 2θ angle  
294 ranging from 5° to 59.98° with a step size of 0.02 and 2750 number of points. The  
295 freeze-dried CNC powders were placed on the sample holder and leveled to obtain  
296 uniform X-ray exposure.

297 The NMR analysis was used to provide the relative masses of crystalline and  
298 amorphous material. Gaussian function was used to perform the deconvolution of  
299 the C4 peaks. CI is calculated by dividing the area of the crystalline peak (integrating  
300 the peak from 87 to 93 ppm) by the total area assigned to the C4 peaks (integrating  
301 the region from 80 to 93 ppm).

302 XRD diffraction were done to determine the crystal type (polymorph). Diffraction  
303 patterns from cellulose Iα and Iβ were calculated based on the published atomic

304 coordinates and unit cell dimension contained in modified “crystal information  
305 files”(cif). Diffraction intensities, output by Mercury program from the Cambridge  
306 Crystallographic Data Centre, has been compared with the experimental data  
307 (French, 2014, Nishiyama et al., 2012).

### 308 *2.7 Thermogravimetric analysis (TGA)*

309 TGA was carried out to determine the thermal stability of the different kinds of  
310 CNC by employing a thermogravimetric analyser Perkin Elmer, TGA 4000.  
311 Samples were heated from 30°C to 800°C under air or nitrogen atmosphere at a  
312 heating rate of 10°Cmin<sup>-1</sup>; three replication were done for each CNCs type.

### 313 *2.8 Coating process*

314 A 7% wt CNCs water dispersion (pH = 8) was coated onto PET 12 µm film,  
315 according to ASTM D823-07, practice C. After activation of the external side of  
316 the substrate by using a corona treater, (Arcotech GmbH, Monsheim, Germany),  
317 the CNCs solution was coated by an automatic film applicator (model 1137, Sheen  
318 Instruments, Kingston, UK) at a constant speed of 2.5 mm s<sup>-1</sup>. Water was  
319 evaporated using a constant mild air flow (25±0.3 °C for 5 minutes).

### 320 *2.9 Transparency, Haze and Water Resistance of the coatings*

321 The transmittance of the sample was measured at 550 nm, according to the ASTM  
322 D 1746-70, by means of a Perkin-Elmer L650 UV-VIS spectro-photometer. Haze  
323 (%) was measured in accordance with ASTM D 1003-61 with the same instrument  
324 equipped with a 150 mm integrating sphere. Each sample was replicated three  
325 times, by analyzing four spots for each replica. The moisture sensitivity of the  
326 hydrophilic coatings was done, by using an empirical test, measuring the weight  
327 losses after 4 days of immersion in a water bath at 37 ± 0.5 °C, of ten samples

328 (diameter 12 mm) cut from the two CNCs coated PET films. Samples of the two  
329 kinds of CNCs were submerged in distilled water, avoiding any floating then wiped  
330 up, dried and weighed to measure the weight loss (%).

331

### 332 *2.10 Thickness*

333 The thickness of the two different CNCs coatings were measured **analyzing the**  
334 **cross section by Scanning Electron Microscopy (SEM)**. Scanning electron  
335 microscopy images were obtained from a Sigma Field Emission microscope (Carl  
336 Zeiss Microscopy, LLC) at accelerating 5 kV voltage and 6 mm working distance,  
337 with a 30 m width slit. The samples were first gold sputtered (Sputtering Polaron E  
338 5100) for 30 s (rate 1 nm s<sup>-1</sup>) with argon and 18 mA current intensity.

### 339 *2.11 Oxygen Permeability measurements*

340 The oxygen permeability (PO<sub>2</sub>) of CNCs coated plastic films were assessed (mL  
341 m<sup>-2</sup> d<sup>-1</sup> bar<sup>-1</sup>) by isostatic method (Multiperm, Extra\_Solution S.r.l. Capannori  
342 (LU), Italy) at 23°C and two different relative humidity values (0% and 50% RH),  
343 complying with ASTM D-3985. The oxygen permeability coefficients of the CNCs  
344 coating alone (i.e., KPO<sub>2</sub> of the coating) was calculated using the following  
345 equation (Crank 1979) and assuming that the substrate surface (PET film) does not  
346 interact with the CNCs coating above or that the interface between them, negligibly  
347 affects the final permeation measure.

$$348 \quad \frac{L}{KPO_2(\text{coating})} = \frac{1}{PO_2(\text{coated film})} - \frac{1}{PO_2(\text{bare film})}$$

349

350

### 351 *2.12 Contact angles and surface energies*

352 Self-standing films of the two different CNCs were obtained by casting, leaving  
 353 their suspension evaporate at pH 7 for one night at 30°C in Petri dishes Ø 9 cm.  
 354 Their surface free energies (SFE) were achieved by measuring static contact angles  
 355 of polar Milli-Q water (18.3 MΩ cm) and apolar diiodomethane (99%, Sigma  
 356 Aldrich), using OCA 15 Plus angle goniometer (Data Physics Instruments GmbH,  
 357 Filderstadt, Germany), then elaborated by the Owens-Wendt-Rabel and Kaelble  
 358 (OWRK) method (Owens and Wendt 1969; Kaelble 1970). The measurements of  
 359 static contact angles were performed at room temperature, on five different  
 360 positions for each sample; the sessile drop method was used, by gently dropping a  
 361 droplet of  $4.0 \pm 0.5 \mu\text{L}$  of each liquid onto the substrate. The instrument was  
 362 equipped with a high-resolution CCD camera and a high performance digitizing  
 363 adapter. SCA20 and SCA21 software (Data Physics Instruments GmbH,  
 364 Filderstadt, Germany) were used, respectively, for contact angle measurements and  
 365 surface energy calculation. According to the OWRK theory, the SFE is divided into  
 366 two distinct parts, i.e. the polar  $\gamma_s^P$  and dispersive  $\gamma_s^D$ . These components are the  
 367 square values, respectively, of slope and intercept of the following first order  
 368 equation:

$$369 \quad \frac{\gamma_l(1 + \cos \theta)}{2\sqrt{\gamma_l^D}} = \sqrt{\gamma_s^P} \left( \frac{\sqrt{\gamma_l^P}}{\sqrt{\gamma_l^D}} \right) + \sqrt{\gamma_s^D}$$

370 Therefore, knowing the polar and dispersive components ( $\gamma_l^P$ ,  $\gamma_l^D$ ) of at least two  
 371 liquids (the ones used in this work are reported in Table 1), and the corresponding  
 372 apparent contact angles of these liquids onto the solid surface of interest, a linear  
 373 regression permits to estimate the SFE components  $\gamma_s^P$  and  $\gamma_s^D$ .

374 *Table 1 Surface tension parameters of the liquids used in contact angle*  
 375 *determination (in mJ/m<sup>2</sup>) at 20°C (van Oss 2003)*

Liquid	$\gamma_l$	$\gamma_l^D$	$\gamma_l^P$
Water	72.8	21.8	51
Diiodomethane	50.8	50.8	0

376

### 377 *2.13 Coefficient of Friction*

378 The static ( $\mu_S$ ) and dynamic ( $\mu_D$ ) friction coefficients (COF) were measured by a  
379 dynamometer (model Z005, Zwick Roell, Ulm, Germany), according to the  
380 standard method ASTM D 1894-87. Firstly, the uncoated side of CNCs coated film  
381 was attached on a specific sled (6.2×6.2 cm<sup>2</sup>, 197.99 g), while the un-coated film  
382 was covered on the sliding plane (exposing the un-treated side). Then the sled was  
383 connected to the force sensor of dynamometer and was horizontally pulled by the  
384 instrument on the covered sliding plane. The raw data (pulling force) were recorded  
385 and analyzed by software TestXpert V10.11 (Zwick Roell, Ulm, Germany).

386

## 387 **3. RESULTS**

### 388 *3.1 CNCs characterization*

389 The two different processes used on the same batch of cotton linters **were able to**  
390 **give cellulose nanocrystals that were characterized to determine the differences of**  
391 **CNCs obtained.**

392 The CNCs were characterized in terms of morphology with TEM (Fig. 1a; Fig 1b)  
393 and hydrodynamic dimension distribution (DLS), (Fig. 2). Electron microscopies  
394 show quite similar rod-like shapes with comparable rod diameters (Table 2) for  
395 CNCs obtained by sulfuric acid and APS treatment. On the other hand a 10%  
396 difference in rod length, and around 20% aspect ratio and PDI are detected. The  
397 higher values were measured for the CNCs achieved through the APS process.

398 **Fig. 1a** Transmission Electron Micrograph (TEM) of cotton linters nanocrystals  
 399 obtained by APS

400 **Fig. 1b** Transmission Electron Micrograph (TEM) of cotton linters nanocrystals  
 401 obtained by H<sub>2</sub>SO<sub>4</sub>

402 **Fig. 2** CNCs hydrodynamic diameter distributions obtained with DLS

403

404 The fact that CNCs are not spherical poses some issues on the CNCs diameter  
 405 calculated by DLS. DLS analyzes the data in spherical approximation,  
 406 mathematically treating the CNCs as spheres moving with Brownian motion  
 407 independently from their real physical morphology. Particularly, when a rod-like  
 408 particle is subjected to Brownian motion, it will be dragged along and rotate, as  
 409 well as for a spherical particle. Differently from spheres, the hydrodynamic stresses  
 410 will depend on the relative orientation of the rods, causing an anisotropic motion of  
 411 the scatterer (Mewis and Wegner 2012). Prolated rod-like structures of length L  
 412 are detected by DLS as equivalent Brownian spheres with a smaller average  
 413 diameter (Kroeger et al. 2007). The average TEM dimension matches the DLS  
 414 measured size distribution (Table 2 and Fig. 2), stressing the good overlap between  
 415 size distribution in CNCs solution and electron micrographies (EM) of drop-casted  
 416 CNCs. Such an average size persistence in presence of strong capillary forces  
 417 associated to drying and absorption before EM measurements underlines the  
 418 stability of the morphology of both the CNCs obtained (Kralchevsky and Nagayama  
 419 1994).

420 *Table 2 TEM/Image and hydrodynamic size distribution of dispersed CNC.*

CNC	TEM-Image ProPlus			DLS	
	Length (nm)	Diameter (nm)	L/d	Nanocrystal diameter in uniform	PDI*



				spherical approximation (nm)	
CNC <sub>H<sub>2</sub>SO<sub>4</sub></sub>	110 ±47	6.7 ± 2.3	16.4 ± 8.9	80.8	0.19
CNC <sub>APS</sub>	121 ± 46	6.2 ± 0.9	19.7 ± 8.0	101.2	0.23

421 \* polydispersity index, defined as  $PDI = (\sigma/D)^2$ , is a measure of the width of  
 422 particle size distribution

423 The length of the nanocrystals, in particular, can be relevant in the networking  
 424 consolidation during the coating process. The similar values and the uncertainty of  
 425 the measures of the aspect ratio of crystals from the two preparations leads to  
 426 assume similar dimensions of the crystals. Other important analyses for the goal of  
 427 this research are the chemical indexes assessed by XRD, NMR, FTIR and  
 428 conductometric titrations. NMR analysis with deconvolution based on Gaussian  
 429 Equation is still often used to interpret the diffraction profile to provide the relative  
 430 masses of crystalline and amorphous material in a given sample (Nishiyama et al.  
 431 2013). In this specific case the values are 62.6±1.1 % for CNC<sub>H<sub>2</sub>SO<sub>4</sub></sub> and 63.8±1.2%  
 432 for CNC<sub>APS</sub> therefore no significant difference in crystallinity content is present.

433 More interesting is the analyses of the XRD diffraction pattern of our experimental  
 434 data compared with the powder diffraction patterns form cellulose I $\alpha$  and I $\beta$  based  
 435 on the published atomic coordinates and unit cell dimension contained in modified  
 436 “crystal information files”(cif) calculated with Mercury Software. The powder  
 437 diffraction patterns are reported in Figure 3.

438 **Fig.3.** Powder diffraction patterns calculated with Mercury software based on the  
 439 cellulose I $\beta$  crystal structure and experimental data obtained by CNCs from APS  
 440 and from H<sub>2</sub>SO<sub>4</sub>.

441 Because of the strong oxidative potential of the APS treatment, an essential  
 442 characterization of the two different CNCs produced is related to the oxidation  
 443 degree and the assessment of the charge density. Both FTIR spectra and  
 444 conductometric titrations were carried out for this purpose and the overall results  
 445 obtained are reported in Table 3. FTIR spectra of APS CNCs (Fig. 4) clearly show  
 446 the typical absorption bands of carboxylic groups. **The two peaks recognizable in**  
 447 **the inset of Figure 4 are referable, according to Lam et al. (2013), to C=O stretching**  
 448 **peaks of the carboxylic group ( $1733\text{ cm}^{-1}$ ) and to  $\text{COO}^-\text{NH}_4^+$  ( $1630\text{ cm}^{-1}$ ),**  
 449 **respectively.**

450 **Fig. 4** FTIR spectra and enlargement recorded for raw cotton linters (blue line),  
 451 from CNC obtained by sulphuric acid hydrolysis (black line) and CNC-COOH  
 452 produced by APS treatment (red line)

453

454 **Concentration of COOH groups resulted to be 0.98 mmol/g of cellulose**  
 455 **nanocrystals, leading to an oxidation degree around 0.15. According to Elazzouzi-**  
 456 **Hafraoui et al. (2009) and assuming that all the glucose units on the surface of each**  
 457 **nanocrystalline cellulose particle are completely carboxylated, the charge content**  
 458 **measured is an estimate of nanocrystals diameter between 6 and 10 nm.** The charge  
 459 density that was accounted for APS CNCs is 4.5 times the value obtained for  
 460 sulfuric acid hydrolysis and this achievement seems consistent with the goal of  
 461 producing a suspension that can be casted, as a thin and functional coating, on the  
 462 activated surface of flexible packaging materials.

463

464 *Table 3 Extraction yield (%), degree of oxidation (DO) and charge density of*  
 465 *CNC*

CNC	Yield (%)	DO	COOH content (mmol/g)	Sulfur Content (mmol/g)	Charge density ( $\text{e}/\text{nm}^2$ )
-----	-----------	----	-----------------------	-------------------------	---

		Conductimetric	FT-IR			
CNC H <sub>2</sub> SO <sub>4</sub>	52.7	-	-	-	0.21±0.9	0.32
CNC APS	34.4	0.15	0.16	0.98±0.10	-	1.46

466

467 The results concerning the oxidation degree and the charge densities of the two  
468 different CNCs appear well correlated to the values of contact angles and surface  
469 energies, measured on specimens obtained by casting the cellulose nanocrystals  
470 from their 7% suspension in water (pH = 7), and reported in Table 3. Both the  
471 samples presented water contact angles consistent with high hydrophilicity largely  
472 expected for their cellulosic origin; however the value of sample from APS process  
473 is lower, showing a much higher wettability. Surface free energies (SFE) were  
474 measured using also the static contact angles of apolar diiodomethane, by means of  
475 the Owens-Wendt-Rabel and Kaelble (OWRK) method, and they also showed a  
476 significant difference between the two samples. CNCs from APS process has a  
477 surface free energy which is 13.6% higher than that of CNCs coming from sulfuric  
478 acid hydrolysis of cotton linters: this is mainly due to the polar part of this energy  
479 (32.54 versus 21.71 mN/m), in accordance with the large presence of carboxyl  
480 groups in the cellulose nanocrystals obtained using ammonium persulfate. It is  
481 reasonable to assume that such a high surface energy can be useful in anchoring the  
482 CNCs layer onto a common activated substrate.

483

484 *Table 4: Static contact angles ( $\theta$ ) and Surface Energy (SFE) of CNC in form of*  
485 *thin casted films.*

CNC	$\theta$ Water	$\theta$ DIM	Polar part (mN/m)	Dispersive part (mN/m)	SFE (mN/m)
CNC H <sub>2</sub> SO <sub>4</sub>	45.72±1.69	44.39±1.87	21.72	37.34	59.09

CNC APS	29.29±1.73	49.67±3.23	32.54	34.46	67.01
------------	------------	------------	-------	-------	-------

---

486

487 The yields recorded for the two processes are rather different, showing the APS  
 488 treatment leading just to a 34,4% in comparison with almost 53% of the sulfuric  
 489 acid hydrolysis. It is worth noting that these values are only indicative and related  
 490 to a specific lab scale production process. In particular, they strongly depend on the  
 491 preparation condition and post treatment filtration. The extraction yield should  
 492 correspond to the proportion of crystalline domains of the cellulosic raw materials  
 493 but usually lower yields are obtained. It was supposed that continued action of the  
 494 reactive agents like acids for long time can cause dissolution of cellulose in  
 495 crystallites (Dufresne 2012), or other reaction byproducts.

496 Thermal stability of CNCs was also tested given its importance for thermoplastic  
 497 applications where the processing temperature is often above 200°C. In literature  
 498 different degradation temperature for nanocrystals are reported because the  
 499 degradation temperature depends from different experimental variables (Roman  
 500 and Winter, 2004).

501 In this case (Fig. 5) TGA curves report a small loss (about 6%) from 30°C until  
 502 250°C, where cellulose undergoes to the most important degradation. Even if the  
 503 TGA analysis was performed in the temperature range between 30°C and 800°C,  
 504 only the range from 100°C to 500°C is reported in Figure 5 because this is the zone  
 505 where the differences between the samples are more visible and the behavior is  
 506 more influenced by the CNCs production process and by the initial humidity of the  
 507 samples. During the hydrolysis reaction, for example, the sulfate or hydroxyl group  
 508 are introduced on the surface of the nanoparticles giving at the same time improved  
 509 stability of the aqueous suspension and lower thermal stability.

510 **Fig 5:** TGA plots, from 100°C to 500°C, of CNC from H<sub>2</sub>SO<sub>4</sub> hydrolysis, CNC-  
511 COO-Na<sup>+</sup> in Nitrogen atmosphere and CNC-COO-Na<sup>+</sup> in air

512 Increasing quantity of sulfate and hydroxyl groups led to lower degradation  
513 temperature (Fig.5) and a broader degradation temperature range was observed in  
514 comparison to unhydrolyzed sample as shown in literature (Roman and Winter  
515 2004). In literature is also reported that the -COOH form of CNCs is more stable  
516 than the COONa<sup>+</sup> (Lam et al. 2012); also in our case the COONa<sup>+</sup> form is more  
517 stable in water solution than the COOH form but it is less thermostable. Complete  
518 decomposition of CNCs to volatile products including CO<sub>2</sub> was observed at T >  
519 400°C; this phenomenon could be attributed to the depolymerization and  
520 decomposition of the cellulose chain. The presence of sulfate groups on  
521 nanocrystals brings to charred residue at 350°C. Heating in air causes oxidation of  
522 the hydroxyl groups resulting, as the temperature increases, in the increase of  
523 carbonyl, carboxyl and hydroperoxide groups; also free radicals appear. The  
524 thermal degradation temperature in this case is higher as shown in Fig. 5.

### 525 *3.2 Coated PET film characterization*

526

527 The turbidity of the APS solution used for coating preparation is lower than  
528 the H<sub>2</sub>SO<sub>4</sub> one and this could be related with the surface charge density reported in  
529 Table 3. Indeed, in the case of APS solution, the higher surface charge  
530 density induces a more efficient electrostatic interactions with water (i.e. a tighter  
531 hydrogen bonds network), leading to more stable CNCs dispersion.

532 The nanocrystals were used, in the form of 7% water dispersion at pH 8, as lacquers  
533 for coating the properly corona treated side of thin PET films. The thickness of the  
534 coatings obtained were well below 1 μm but enough to affect the optical properties,  
535 reducing the transparency and increasing the haze (Table 6) in comparison with the

536 uncoated PET film (T% 84.2, Haze 2.8) After solution deposition on the substrate,  
537 the strong capillary and surface forces due to drying and adsorption trigger a  
538 rearrangement of the crystal structure.

539 Cellulose is known to have very high transparency in solid non-porous form. In this  
540 case, we are in presence of a decrease of transparency of the PET film and this  
541 decrease is higher in the case of CNCs from H<sub>2</sub>SO<sub>4</sub> treatment (Table 5). Moreover,  
542 SEM micrographs of the coatings surface, recorded at 1 KK and 100KX  
543 Magnification, showed homogenous surface of the coatings with the presence  
544 of some holes (Figure 6), with a more pronounced roughness in CNCs  
545 H<sub>2</sub>SO<sub>4</sub> coating than in APS that can be correlated with the higher decrease in  
546 transparency of the coating produced with CNCs H<sub>2</sub>SO<sub>4</sub> .

547 **Fig.6:** SEM micrographs at 1KX and 100KX Magnification of the of the coatings  
548 surface produced by CNCs from H<sub>2</sub>SO<sub>4</sub> (up) and CNS form APS (down)  
549 SEM observation of the same sample but in cross section permitted to verify, that  
550 the surface of the coating is homogeneous in thickness and the values of the  
551 thickness for both the coating is around 450±50 nm (Figure 7).

552 **Fig.7** SEM micrographs at 180KX Magnification of the of the cross section of the  
553 films containing the coating of CNCs from H<sub>2</sub>SO<sub>4</sub> (up) and CNS form APS (down)  
554 At the same time, the test of the water resistance showed that APS coating was  
555 removed only for 49.2%, while the sulfuric acid CNCs layer was almost completely  
556 removed (87.4%). Despite its empiricism, the test perceptibly reveals a higher  
557 stability of the APS coating compared to the H<sub>2</sub>SO<sub>4</sub> one. In Table 5, also the  
558 coefficients of friction (COF, both dynamic and static) measured for the two coated  
559 films are reported. The values, pertinent to the sulfuric acid CNCs coating, are quite  
560 similar to the ones obtained in a previous work (Li et al. 2013a), for various films  
561 (OPET, OPP, Cellophane and OPA) coated with the same CNCs. The achievement

562 of similar COF values for different coated films were assumed as an evidence of a  
 563 complete and uniform covering of the substrates. The values obtained for APS  
 564 CNCs coated PET are significantly lower, both as dynamic and static coefficients.  
 565 This achievement can be interpreted as a possible better performance on the  
 566 automatic machineries for converting the coated material or for a potential  
 567 packaging operation, but it also confirms a very good adhesion to the plastic film  
 568 and a compact and uniform coating offered by the cellulose nanocrystals.

569 *Table 5: Optical properties, clarity of the CNCs in water dispersion (7%), water*  
 570 *resistance and coefficients of friction (COF).*

<b>Coating</b>	<b>Clarity (Abs 600 nm)</b>	<b>Haze (%)</b>	<b>Transparency (%)</b>	<b>Water Resistance (% losses)</b>	<b>COF (<math>\mu_D</math>)</b>	<b>COF (<math>\mu_S</math>)</b>
CNCs H <sub>2</sub> SO <sub>4</sub>	3.1±0.1	5.99±0.11	77.48±0.02	87.4±3.0	0.28±0.01	0.31±0.01
CNCs APS	1.8±0.05	6.19±0.10	79.55±0.01	49.2±3.3	0.21±0.01	0.24±0.01

571  
 572  
 573 Owing to the highly hydrophilic nature of these coatings and the results obtained in  
 574 previous researches (Li et al. 2013a), the most promising property of such CNC  
 575 coatings is gas barrier. Therefore, the oxygen permeability was measured at two  
 576 different relative humidity values at room temperature for both the coated PET  
 577 films and the uncoated substrate. The results obtained are presented in Table 6 and  
 578 show a very sharp reduction of gas diffusion through the PET film, once coated by  
 579 the CNCs. To get the same permeability, just increasing the plastic thickness, a 1.5  
 580 mm thick PET film would be necessary to have the same performance offered by  
 581 the sulfuric acid nano-cellulose coating. In the case of APS CNCs coated film, the  
 582 thickness of the “standard” PET sheet having the same permeability should be  
 583 around 8.2 mm. The very high oxygen barrier demonstrated by APS CNCs coating,

584 which is much higher than that of the majority of synthetic barrier resins commonly  
 585 used in food packaging applications, realistically derives from the inherent  
 586 morphological, chemical and physical characteristics of these nanocrystals, which  
 587 lead to low diffusion. The apparent higher moisture sensitivity of CNCs from the  
 588 APS process, which shows a higher increase of permeability when measured at 50%  
 589 RH in comparison with H<sub>2</sub>SO<sub>4</sub> CNCs coated film, is consistent with the higher  
 590 wettability shown by optical contact angle evaluation (Table 4) and can be  
 591 attributed to the higher charge density. In any case, the moisture sensitivity of the  
 592 coating, as happens for EVOH or PVOH oxygen barrier synthetic resins, doesn't  
 593 permit the use of such materials at high relative humidity (80% or higher) and it  
 594 could be overcome by the need of providing a sealable layer, thus polyolefinic and  
 595 moisture barrier, to the possible final laminate in a real application.

596  
 597 *Table 6: Oxygen permeability (PO<sub>2</sub>) and permeability coefficients (KPO<sub>2</sub>) of*  
 598 *CNC coated films and coatings alone.*

Sample	PO <sub>2</sub> (mL m <sup>-2</sup> d <sup>-1</sup> bar <sup>-1</sup> ) 0%RH, 23°C	PO <sub>2</sub> (mL m <sup>-2</sup> d <sup>-1</sup> bar <sup>-1</sup> ) 50%RH, 23°C
PET uncoated film	74.95±1.83	87.96±1.13
CNC H <sub>2</sub> SO <sub>4</sub> coated PET	1.06±0.07	5.99±2.21
CNC APS coated PET	0.17±0.01	3.53±1.92

Sample	KPO <sub>2</sub> (mL μm m <sup>-2</sup> d <sup>-1</sup> bar <sup>-1</sup> ) 0%RH, 23°C	KPO <sub>2</sub> (mL μm m <sup>-2</sup> d <sup>-1</sup> bar <sup>-1</sup> ) 50%RH, 23°C
PET uncoated film	899.4±1.83	1,055±1.13
CNC H <sub>2</sub> SO <sub>4</sub> coating alone	0.48±0.01	2.89±0.01
CNC APS coating alone	0.075±0.01	1.65±0.01



---

599        **4. CONCLUSIONS**

600    The use of ammonium persulfate to obtain cellulose nanocrystals has been initially  
601    proposed in order to perform in one single step a complete fragmentation of various  
602    cellulosic biomasses, in contrast to acid hydrolysis which requires pretreatment  
603    steps for cellulose isolation. This is a very important target that deserves to be fully  
604    explored to valorize largely available, renewable resources. In this paper the  
605    advantage of using this kind of oxidized CNCs for improving the performance of  
606    common food packaging materials, while increasing their possible sustainability,  
607    was proved. Transparency, friction coefficient, wettability of the coating were  
608    always better for the CNCs coating obtained by the APS process, and especially the  
609    oxygen barrier property revealed as a very interesting and promising feature.  
610    Therefore, these advantages must be correlated to the higher charge density (due to  
611    the presence of carboxylic groups), which in turn gave rise to a more performing  
612    coating **and availability of functional groups that can be used for grafting the CNCs**  
613    **to other molecules that could be involved in a lamination process. In fact,** as the  
614    tests performed demonstrated, for its intrinsic nature the hydrophilic coating is very  
615    sensitive to moisture and it is not thermoplastic, thus neither thermo-sealable as  
616    shown in the Differential Scanning Calorimetry analysis (Online Resource 1);  
617    **therefore** such a high performing coating has to be protected by means of a  
618    hydrophobic and sealable polymeric layer in case of a practical application as food  
619    packaging material. Nevertheless this is the same problem that must be faced when  
620    synthetic barrier polymer, such as polyvinyl alcohol (**PVOH**) or ethylene vinyl  
621    alcohol copolymer (EVOH) are used. Because CNCs coating showed oxygen  
622    permeability coefficient, which are lower than the synthetic resins, it can be

623 considered as their possible alternative to increase gas barrier properties, while  
624 reducing the oil resources dependency.

625

626 **Acknowledgements**

627 The authors wish to acknowledge Professors Francesco Demartin, Department of  
628 Chemistry, Dr. Marco Signorelli, DEFENS, University of Milan and Dr. Giorgio  
629 Capretti of INNOVHUB-SSI, Milan, for technical support in analysis and scientific  
630 support.

631

632  
633  
634

## REFERENCES

- 635 Araki J, Wada M, Kuga S. (2000) Steric Stabilization of a Cellulose Microcrystal  
636 Suspension by Poly(ethylene glycol) Grafting. *Langmuir* **17**(1):21-27.  
637 doi:10.1021/la001070m
- 638 Arola S, Tammelin T, Setälä H, Tullila A, Linder MB. (2012) Immobilization-  
639 Stabilization of Proteins on Nanofibrillated Cellulose Derivatives and Their  
640 Bioactive Film Formation. *Biomacromolecules* **13**(3): 594-603. doi:  
641 10.1021/Bm201676q
- 642 Beck-Candanedo S, Roman M, Gray DG. (2015) Effect of Reaction Conditions on  
643 the Properties and Behavior of Wood Cellulose Nanocrystal Suspensions.  
644 *Biomacromolecules* **6**(2):1048-1054. doi:10.1021/bm049300p
- 645 Beer F, Muller J. (1962) Process for the production of caro's acid salts and solutions  
646 thereof. In Google Patents. <https://www.google.com/patents/US3036885>.  
647 Accessed 08 July 2015
- 648 Berglund LA. (2005) Cellulose-based nanocomposites. In: Mohanty, A.K., Misra,  
649 M., Drzal, L.T. (eds.) *Natural fibers, biopolymers, and biocomposites*. CRC  
650 Press, Boca Raton, Florida
- 651 Belbekhouche, S. Bras J, Siqueira G, Chappey C Lebrun L, Khelifi B, Marais S  
652 and , Dufresne A. (2011) Water sorption behavior and gas barrier properties  
653 of cellulose whiskers and microfibrils films *Carbohydrate Polymers*  
654 831740–1748
- 655 Berne BJ, Pecora R. (2000) *Dynamic light scattering: with applications to*  
656 *chemistry, biology, and physics*. Courier Corporation, New York
- 657 Bondeson D, Mathew A, Oksman K. (2006) Optimization of the isolation of  
658 nanocrystals from microcrystalline cellulose by acid hydrolysis. *Cellulose*  
659 **13**(2):171-180. doi:10.1007/s10570-006-9061-4
- 660 Cheng M, Qin Z, Liu Y, Qin Y, Li T, Chen L, Zhu M. (2014) Efficient extraction  
661 of carboxylated spherical cellulose nanocrystals with narrow distribution  
662 through hydrolysis of lyocell fibers by using ammonium persulfate as an  
663 oxidant. *Journal of Materials Chemistry A* **2**(1):251-258.  
664 doi:10.1039/C3TA13653A
- 665 Chinga-Carrasco G, Syverud K. (2014) Pretreatment-dependent surface chemistry  
666 of wood nanocellulose for pH-sensitive hydrogels. *Journal of Biomaterials*  
667 *Applications* **29**(3), 423-432. doi:10.1177/0885328214531511
- 668 Crank J. (1979) *The mathematics of diffusion*. Oxford university press
- 669 Dong XM, Kimura T, Revol JF, Gray DG. (1996) Effects of Ionic Strength on the  
670 Isotropic–Chiral Nematic Phase Transition of Suspensions of Cellulose  
671 Crystallites. *Langmuir* **12**(8):2076-2082. doi:10.1021/la950133b
- 672 Dufresne A. (2012) *Nanocellulose: from nature to high performance tailored*  
673 *materials*. Walter de Gruyter, Berlin
- 674 Elazzouzi-Hafraoui S, Nishiyama Y, Putaux JL, Heux L, Dubreuil F, Rochas C.  
675 (2008) The shape and size distribution of crystalline nanoparticles prepared  
676 by acid hydrolysis of native cellulose. *Biomacromolecules* **9**(1):57-65.  
677 doi:10.1021/Bm700769p
- 678 Espino E, Cakir M, Domenek S, Román-Gutiérrez AD, Belgacem N, Bras J. (2014)  
679 Isolation and characterization of cellulose nanocrystal sfrom industrial by-

680 products of Agave tequilana and barley. *Industrial Crops and Products*  
681 **62**:552-559

682 Favier V, Canova GR, Cavallé JY, Chanzy H, Dufresne A, Gauthier C. (1995)  
683 Nanocomposite materials from latex and cellulose whiskers. *Polym Advan*  
684 *Technol* **6**(5):351-355. doi:10.1002/pat.1995.220060514

685 Filpponen I. (2009) The Synthetic Strategies for Unique Properties in Cellulose  
686 Nanocrystal Materials. Dissertation, North Carolina State University

687 Filson PB, Dawson-Andoh BE. (2009) Sono-chemical preparation of cellulose  
688 nanocrystals from lignocellulose derived materials. *Bioresource Technol*  
689 **100**(7):2259-2264. doi:10.1016/j.biortech.2008.09.062

690 French, A D. (2014) Idealized powder diffraction patterns for cellulose polymorphs.  
691 *Cellulose* **21**:885-896

692 Frounchi M, Dourbash A. (2009) Oxygen Barrier Properties of Poly(ethylene  
693 terephthalate) Nanocomposite Films. *Macromol Mater Eng* **294**(1):68-74.  
694 doi:10.1002/mame.200800238

695 Galland S, Berthold F, Prakobna K, Berglund LA. (2015) Holocellulose Nanofibers  
696 of high molar mass and small diameter for high-strength nanopaper.  
697 *Biomacromolecules* **16**:2427-2435. doi:10.1021/acs.biomac.5b00678

698 Gall JF, Church GL, Brown RL. (1943) Solubility of Ammonium Persulfate in  
699 Water and in Solutions of Sulfuric Acid and Ammonium Sulfate. *The*  
700 *Journal of Physical Chemistry* **47**(9):645-649. doi:10.1021/j150432a003

701 Garvey CJ, Parker IH, Simon GP. (2005) On the Interpretation of X-Ray Diffraction  
702 Powder Patterns in Terms of the Nanostructure of Cellulose I Fibres.  
703 *Macromol Chem Phys* **206**(15):1568-1575. doi:10.1002/macp.200500008

704 Habibi Y, Chanzy H, Vignon MR. (2006) TEMPO-mediated surface oxidation of  
705 cellulose whiskers. *Cellulose* **13**(6):679-687. doi:10.1007/s10570-006-  
706 9075-y

707 Håkansson H, Ahlgren P. (2005) Acid hydrolysis of some industrial pulps: effect  
708 of hydrolysis conditions and raw material. *Cellulose* **12**(2):177-183.  
709 doi:10.1007/s10570-004-1038-6

710 Elazzouzi-Hafraoui S, Putaux JL, Heux L. (2009) Self-assembling and chiral  
711 nematic properties of organophilic cellulose nanocrystals. *J. Phys Chem B*  
712 **113**(32):11069-11075

713 Hult EL, Iversen T, Sugiyama J. (2003) Characterization of the supermolecular  
714 structure of cellulose in wood pulp fibres. *Cellulose* **10**(2):103-110.  
715 doi:10.1023/A:1024080700873

716 Ifuku S, Tsuji M, Morimoto M, Saimoto H, Yano H. (2009) Synthesis of silver  
717 nanoparticles templated by TEMPO-mediated oxidized bacterial cellulose  
718 nanofibers. *Biomacromolecules* **10**(9):2714-2717. doi:10.1021/bm9006979

719 Iwamoto S, Abe K, Yano H. (2008) The Effect of Hemi- celluloses on Wood Pulp  
720 Nanofibrillation and Nanofiber Network Characteristics.  
721 *Biomacromolecules* **9**(3):1022-1026. doi:10.1021/bm701157n

722 Jayakrishnan A, Shah DO. (1984) Phase-transfer-catalyzed polymerization of  
723 acrylonitrile. *J Appl Polym Sci* **29**(9):2937-2940.  
724 doi:10.1002/app.1984.070290921

725 Kaelble DH. (1970) Dispersion-Polar Surface Tension Properties of Organic Solids.  
726 *The Journal of Adhesion* **2**(2):66-81. doi:10.1080/0021846708544582

727 Kolthoff I, Miller I. (1951) The Chemistry of Persulfate. I. The Kinetics and  
728 Mechanism of the Decomposition of the Persulfate Ion in Aqueous Medium.  
729 *Journal of the American Chemical Society* **73**(7):3055-3059

- 730 Kralchevsky PA, Nagayama K. (1994) Capillary forces between colloidal particles.  
731 *Langmuir* **10**(1):23-36
- 732 Kroeger A, Deimede V, Belack J, Lieberwirth I, Fytas G, Wegner G. (2007)  
733 Equilibrium length and shape of rodlike polyelectrolyte micelles in dilute  
734 aqueous solutions. *Macromolecules* **40**(1):105-115
- 735 Lam E, Leung ACW, Liu Y, Majid E, Hrapovic S, Male KB, Luong JHT. (2013)  
736 Green Strategy Guided by Raman Spectroscopy for the Synthesis of  
737 Ammonium Carboxylated Nanocrystalline Cellulose and the Recovery of  
738 Byproducts. *ACS Sustainable Chemistry & Engineering* **1**(2):278-283.  
739 doi:10.1021/sc3001367
- 740 Lasoski SW, Cobbs WH. (1959) Moisture permeability of polymers. I. Role of  
741 crystallinity and orientation. *Journal of Polymer Science* **36**(130):21-33.  
742 doi:10.1002/pol.1959.1203613003
- 743 Leung A, Hrapovic S, Lam E, Liu YL, Male KB, Mahmoud KA, Luong JHT.  
744 (2011) Characteristics and Properties of Carboxylated Cellulose  
745 Nanocrystals Prepared from a Novel One-Step Procedure. *Small* **7**(3):302-  
746 305. doi:10.1002/sml.201001715
- 747 Leung CW, Luong JHT, Hrapovic S, Lam E, Liu Y, Male KB, Mahmoud K, Rho  
748 D. (2012) Cellulose nanocrystals from renewable biomass. In. Google  
749 Patents <https://www.google.com/patents/US8900706>. Accessed 08 July  
750 2015
- 751 Li F, Biagioni P, Bollani M, Maccagnan A, Piergiovanni L. (2013a) Multi-  
752 functional coating of cellulose nanocrystals for flexible packaging  
753 applications. *Cellulose* **20** (5):2491-2504. doi:10.1007/s10570-013-0015-3
- 754 Li F, Biagioni P, Finazzi M, Tavazzi S, Piergiovanni L. (2013b) Tunable green  
755 oxygen barrier through layer-by-layer self-assembly of chitosan and  
756 cellulose nanocrystals. *Carbohydr Polym* **92**(2):2128-2134.  
757 doi:10.1016/j.carbpol.2012.11.091
- 758 Li F, Mascheroni E, Piergiovanni L. (2015) The Potential of NanoCellulose in the  
759 Packaging Field: A Review. *Packaging Technology and Science*, **28**(6):  
760 475-508. doi:10.1002/pts.2121
- 761 Liimatainen H, Visanko M, Sirvio JA, Hormi OEO, Niinimäki J. (2012)  
762 Enhancement of the Nanofibrillation of Wood Cellulose through Sequential  
763 Periodate-Chlorite Oxidation. *Biomacromolecules* **13**(5):1592-1597.  
764 doi:10.1021/Bm300319m
- 765 Mewis J, Wagner NJ. (2012) Colloidal suspension rheology. Cambridge University  
766 Press
- 767 Miller KS, Krochta JM. (1997) Oxygen and aroma barrier properties of edible  
768 films: A review. *Trends in Food Science & Technology* **8**(7):228-237.  
769 doi:10.1016/S0924-2244(97)01051-0
- 770 Moon RJ, Martini A, Nairn J, Simonsen J, Youngblood J. (2011) Cellulose  
771 nanomaterials review: structure, properties and nanocomposites. *Chem Soc*  
772 *Rev* **40**(7):3941-3994. doi:10.1039/c0cs00108b
- 773 Nakagaito A, Yano H. (2004) The Effect of Morphological Changes from Pulp  
774 Fiber Towards Nano-Scale Fibrillated Cellulose on the Mechanical  
775 Properties of High-Strength Plant Fiber Based Composites. *Applied Physics*  
776 *A: Materials Science and Processing* **78**(4):547-552. doi:10.1007/s00339-  
777 003-2453-5
- 778 Nickerson RF, Habrle JA. (1947) Cellulose Intercrystalline Structure. *Industrial &*  
779 *Engineering Chemistry* **39**(11):1507-1512. doi:10.1021/ie50455a024.

- 780 Nishiyama Y. (2009) Structure and properties of the cellulose microfibril. *Journal*  
781 *of Wood Science* 55: 241-249.
- 782 Nishiyama Y, Johnson GP and French AD. (2012) Diffraction from nonperiodic  
783 models of cellulose crystals, *Cellulose* 19:319-336
- 784 Nishiyama Y, Kim UJ, Kim DY, Katsumata KS, May RP, Lagan P. (2003).  
785 Periodic disorder along ramie cellulose microfibrils. *Biomacromolecules*,:  
786 4, 1013-1017
- 787 Okano T, Kuga S, Wada M, Araki J, Ikuina JP. (1999) Nisshin Oil Mills Ltd. Japan  
788 Patent JP 98/151052
- 789 Owens DK, Wendt RC. (1969) Estimation of the surface free energy of polymers.  
790 *J Appl Polym Sci* 13(8): 1741-1747. doi:10.1002/app.1969.070130815
- 791 Paakko MKN, Ankerfors M, Kosonen H, Nykanen A, Ahola S, Osterberg M,  
792 Ruokolainen J, Laine J, Larsson PT, Ikkala O, Lindstrom T. (2007)  
793 Enzymatic hydrolysis combined with mechanical shearing and high-  
794 pressure homogenization for nanoscale cellulose fibrils and strong gels.  
795 *Biomacromolecules* 8(6):1934-1941. doi:10.1021/Bm061215p
- 796 Park S, Baker JO, Himmel ME, Parilla PA, Johnson DK. (2010) Cellulose  
797 crystallinity index: measurement techniques and their impact on interpreting  
798 cellulase performance. *Biotechnology for Biofuels* 3:10
- 799 Peng C, Wenshuai C, Yixing L. (2010) Method for Preparing Nanometer Cellulose  
800 Fiber through Combining Ultrasound and Highpressure Homogenization  
801 Treatment. State Intellectual Property Office (SIPO) CN 101851295A
- 802 Pines A, Gibby MG, Waugh JS. (1973) Proton-enhanced NMR of dilute spins in  
803 solids. *The Journal of Chemical Physics* 59(2):569-590.  
804 doi:10.1063/1.1680061
- 805 Qi A, Chan P, Ho J, Rajapaksa A, Friend J, Yeo L. (2011) Template-free synthesis  
806 and encapsulation technique for layer-by-layer polymer nanocarrier  
807 fabrication. *ACS Nano* 5(12):9583-9591. doi:10.1021/nn202833n
- 808 Rebouillat S, Pla F. (2013) State of the Art Manufacturing and Engineering of  
809 Nanocellulose: A Review of Available Data and Industrial Applications.  
810 *Journal of Biomaterials and Nanobiotechnology* 4(2): 165-188.  
811 doi:10.4236/jbnb.2013.42022
- 812 Roman M, Winter WT. (2004) Effect of Sulfate Groups from Sulfuric Acid  
813 Hydrolysis on the Thermal Degradation Behavior of Bacterial Cellulose.  
814 *Biomacromolecules* 5(5):1671-1677. doi:10.1021/bm034519+
- 815 Saito T, Isogai A. (2007) Wet strength improvement of TEMPO-oxidized cellulose  
816 sheets prepared with cationic polymers. *Ind Eng Chem Res* 46(3):773-780.  
817 doi:10.1021/Ie0611608
- 818 Saito T, Kimura S, Nishiyama Y, Isogai A. (2007) Cellulose nanofibers prepared  
819 by TEMPO-mediated oxidation of native cellulose. *Biomacromolecules*  
820 8(8):2485-2491. doi:10.1021/Bm0703970
- 821 Salame M. (1989) The use of barrier polymers in food and beverage packaging, vol.  
822 1. Plastic film technology. Technologic Publishing Co. Inc., Lancaster USA
- 823 Segal L, Creely JJ, Martin AE, Conrad CM. (1959) An Empirical Method for  
824 Estimating the Degree of Crystallinity of Native Cellulose Using the X-Ray  
825 Diffractometer. *Textile Research Journal* 29(10): 786-794.  
826 doi:10.1177/004051755902901003
- 827 Sinha Ray S, Okamoto M. (2003) Polymer/layered silicate nanocomposites: a  
828 review from preparation to processing. *Prog Polym Sci* 28(11):1539-1641.  
829 doi:10.1016/j.progpolymsci.2003.08.002

830 Siro I, Plackett D. (2010) Microfibrillated cellulose and new nanocomposite  
831 materials: a review. *Cellulose* **17**(3):459-494. doi:10.1007/s10570-010-  
832 9405-y

833 Spence K, Venditti RA, Rojas O, Pawlak J. (2011) Effects of lignin on processing  
834 and properties of microfibrillated cellulose. *Abstr Pap Am Chem S* **241**

835 Spence KL, Venditti RA, Habibi Y, Rojas OJ, Pawlak JJ. (2010a) The effect of  
836 chemical composition on microfibrillar cellulose films from wood pulps:  
837 Mechanical processing and physical properties. *Bioresource Technol*  
838 **101**(15):5961-5968. doi:10.1016/j.biortech.2010.02.104

839 Spence KL, Venditti RA, Rojas OJ, Habibi Y, Pawlak J. (2010b) The effect of  
840 chemical composition on microfibrillar cellulose films from wood pulps:  
841 water interactions and physical properties for packaging applications.  
842 *Cellulose* **17**(4):835-848. doi:10.1007/s10570-010-9424-8

843 Springer EL, Minor JL. (1991) Delignification of lignocellulosic materials with  
844 monoperoxysulfuric acid. United States Patent 5,004,523 issued Apr. 2,  
845 1991

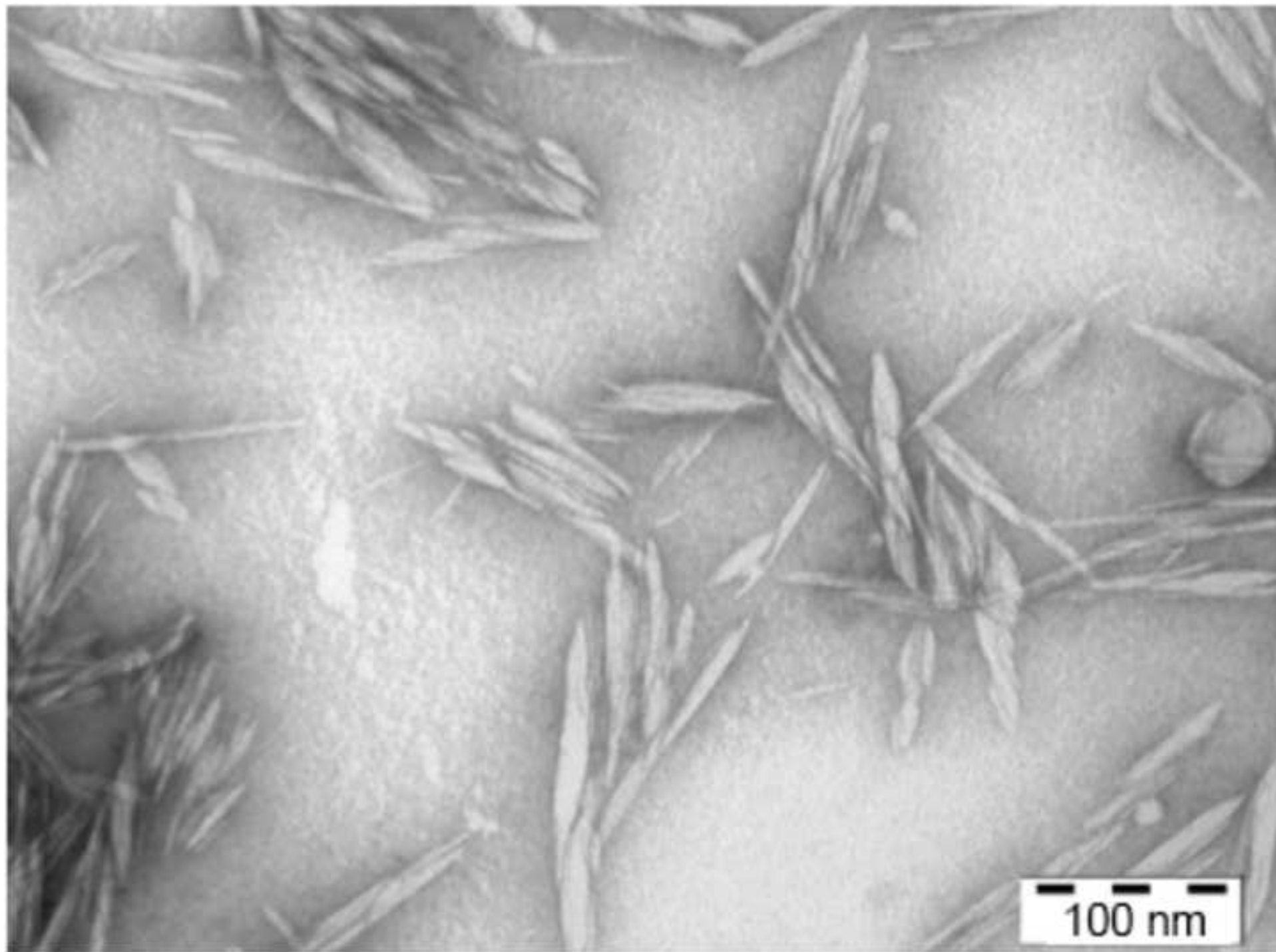
846 Turrentine JW. (1906) Action of Ammonium Persulphate on Metals. *The Journal*  
847 *of Physical Chemistry* **11**(8):623-631. doi:10.1021/j150089a004

848 van Oss CJ. (2003) Long-range and short-range mechanisms of hydrophobic  
849 attraction and hydrophilic repulsion in specific and aspecific interactions.  
850 *Journal of Molecular Recognition* **16**(4):177-190

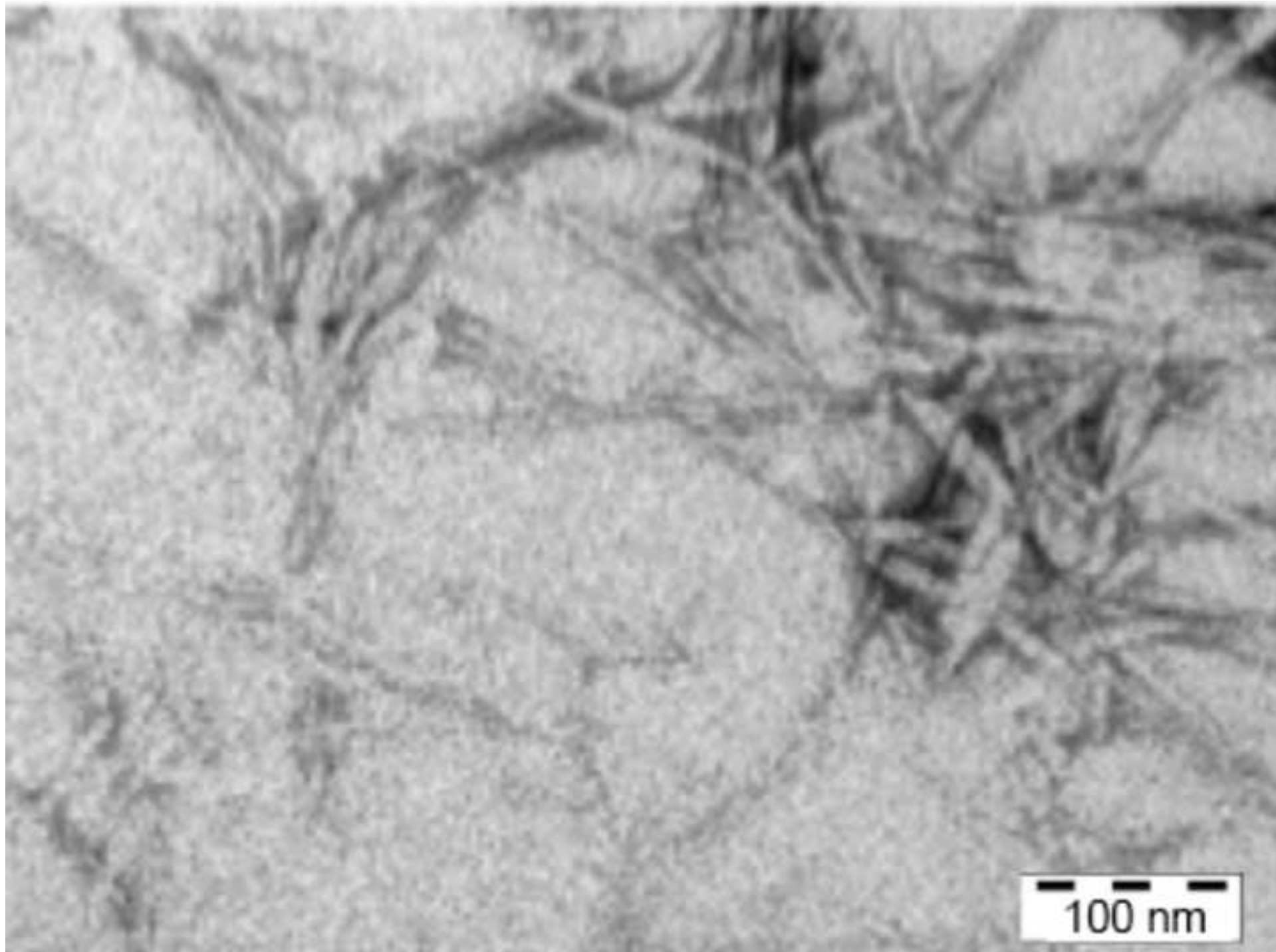
851 Yang H, Alam MdN, van de Ven TGM. (2013) Highhli cristalline charged  
852 nanocrystalline cellulose and dicarboxylated cellulose from periodate and  
853 chlorite oxidized cellulose fibers. *Cellulose* **20**:1865-1875.  
854 doi:10.1007/s10570-013-9966-7

855

856







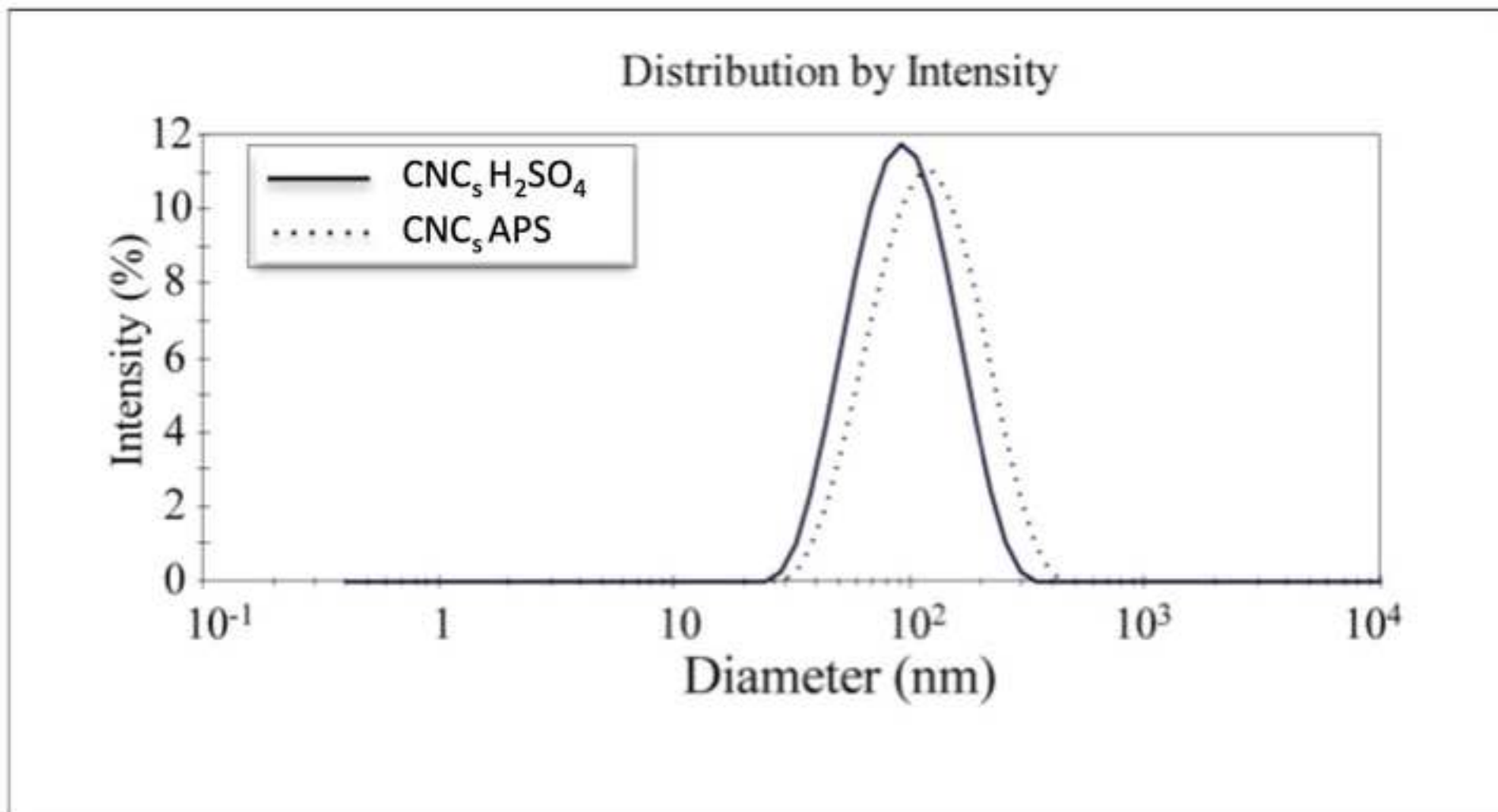
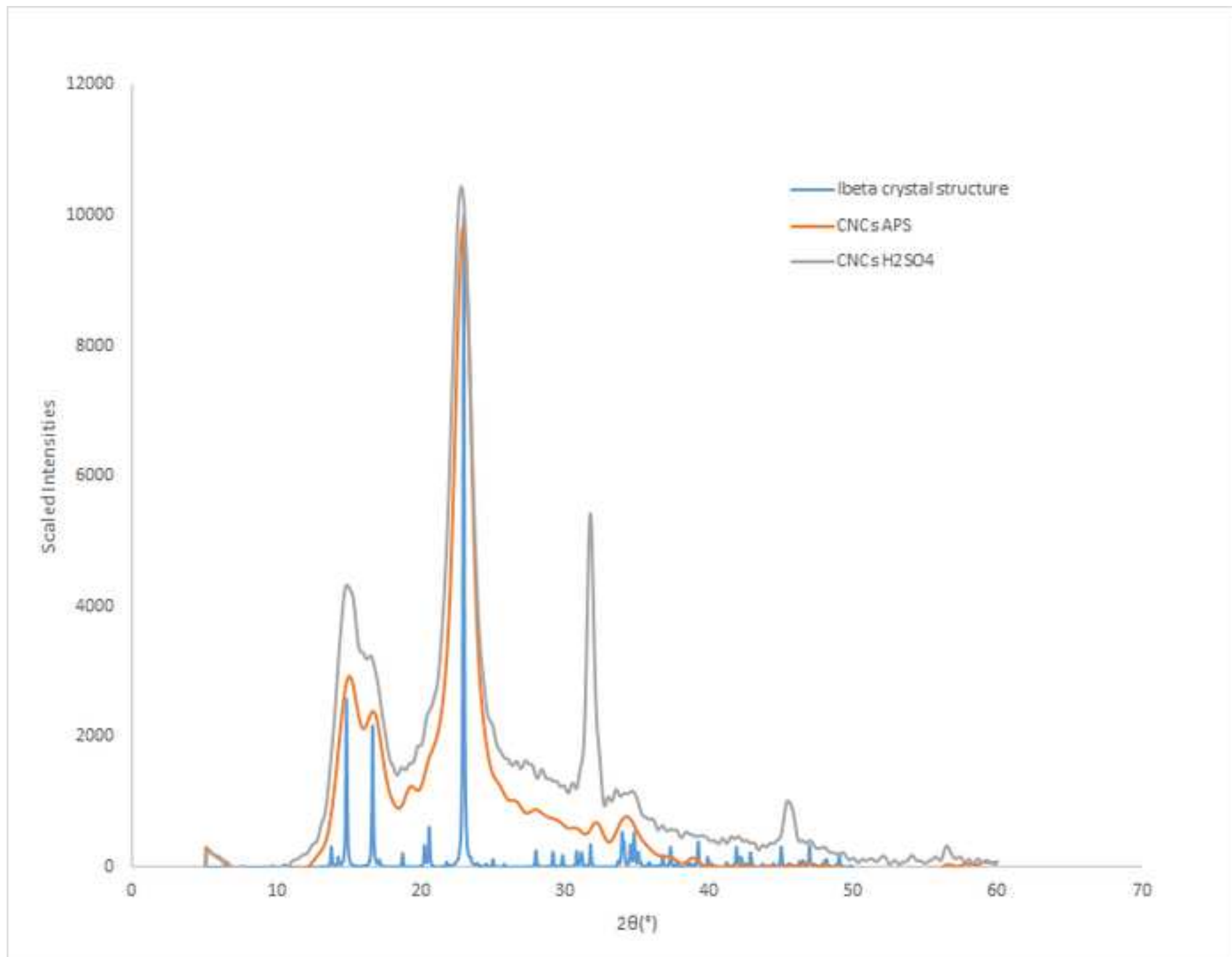
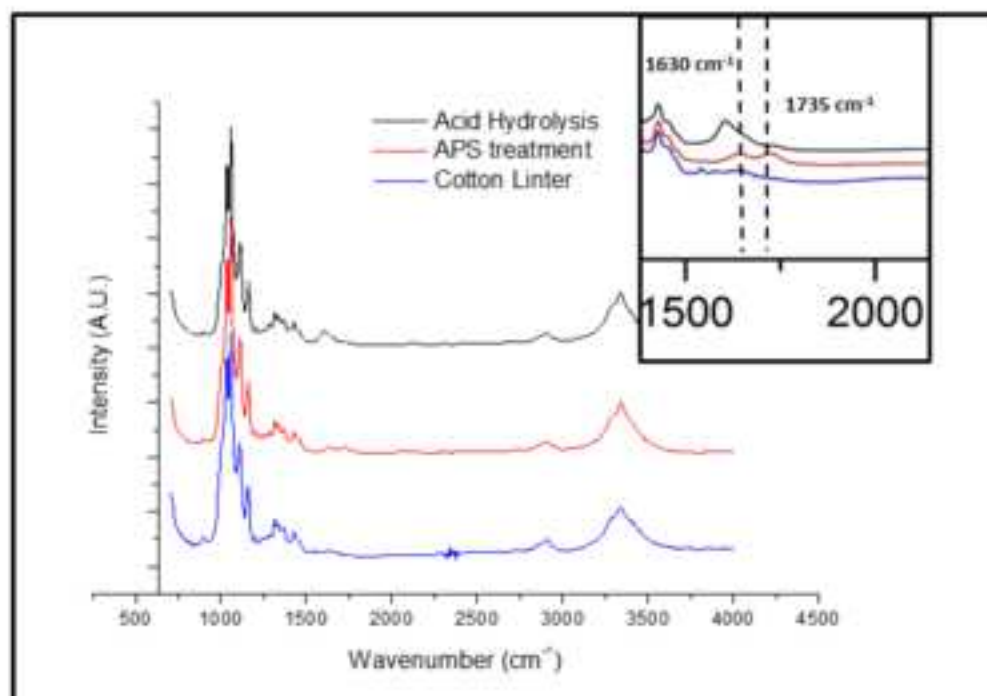
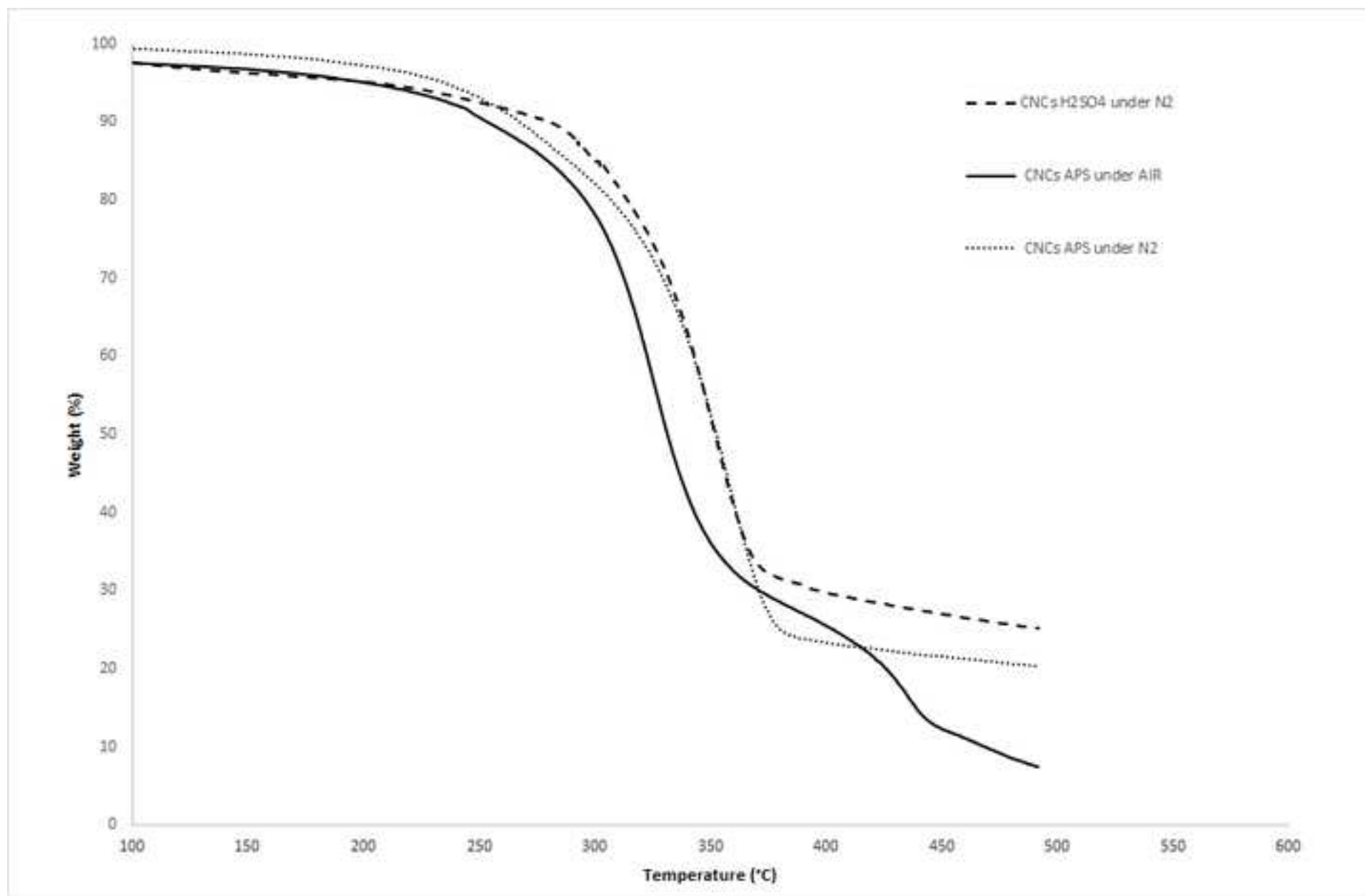
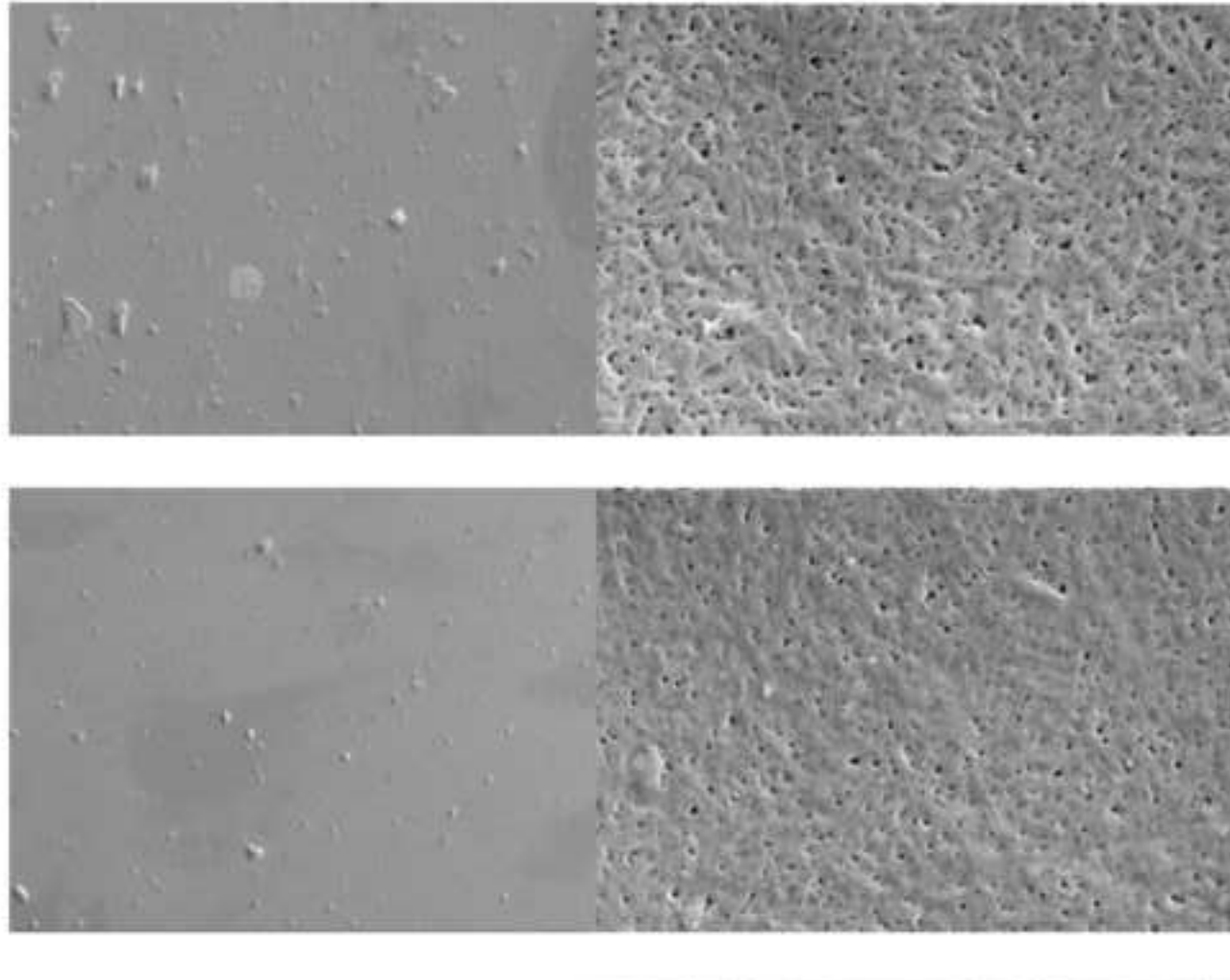


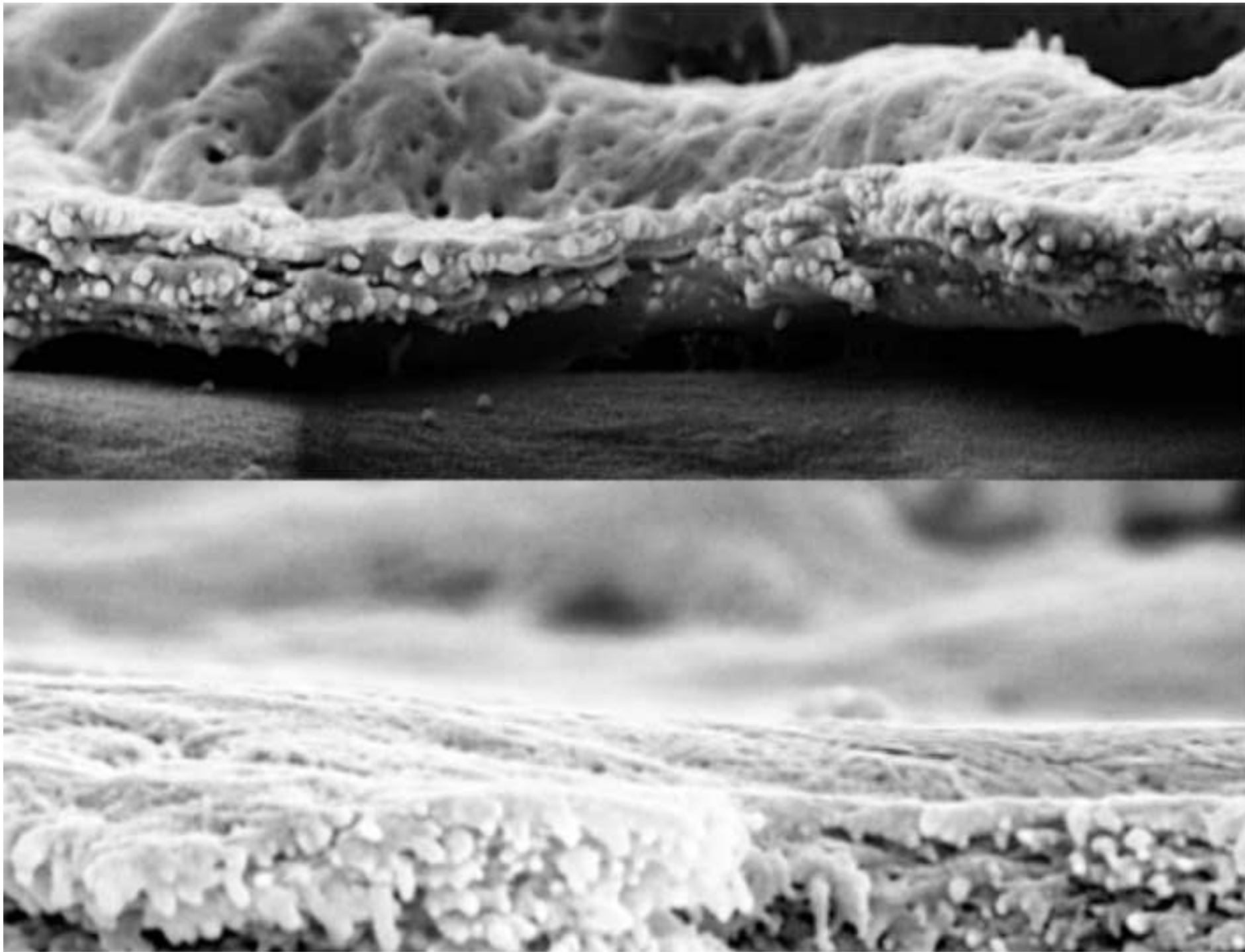
Figure 3

















Click here to access/download  
**Supplementary Material**  
Answer to the reviewers.docx

